

PCA R&D Serial No. 2581

Soil Stabilization Field Trial

by K. P. George

KEYWORDS

additives, cement, concrete, CMT, cement treated material, precut, prepacked, soil stabilization

ABSTRACT

A five-year study was initiated seeking materials/additives and procedures that help to mitigate crack susceptibility in cement-treated material (CTM). A field test program of six 305-m (1000-ft) test sections was implemented in August 2000. The following additives/procedures were included for investigation:

- 5.5% cement additive (control section); design based on a reduced strength criteria.
- 5.5% cement precracked 24 to 48 hours after finishing.
- 5.5% cement precut (grooved) every 3 m (10 ft).
- 3.5% cement with 8% fly ash (CFA).
- 6% ground granulated blast furnace slag (GGBFS) with 2% lime admixture (LGBFS).
- 3% lime and 12% fly ash; stabilization technique used by MDOT (LFA).

The first interim report covering the first phase of investigation/monitoring during the 28-day period was submitted on April 21, 2001. Two layers of hot mix asphalt (HMA) – 110-mm (4.5-in.) base, 60-mm (2.25-in.) polymer modified binder – were placed over the stabilized layer beginning September 21, 2000, followed by the second field monitoring on November 13, 2001. Field tests included deflection tests employing Falling Weight Deflectometer (FWD), retrieval of 100-mm (4-in.) cores for compression tests, and a manual crack survey. The results were presented in Interim Report II. On June 16, 2003, (nominally three years) the test sections were monitored again, also with a deflection test employing FWD and a manual crack survey. Prior to the June 2003 survey, a 50-mm (2-in.) polymer modified surface course was placed, with the road opening to traffic on July 8, 2002.

Nominally five years after construction, again deflection tests deploying FWD (December 1, 2004), compression tests on 102-mm (4-in.) cores, and a manual crack survey (March 8, 2005) were conducted. Presented in this final report are (i) the results of the deflection analysis and moduli of layers, (ii) the compressive strength results of 102-mm (4-in.) diameter cores, and (iii) the crack survey results.

Backcalculation of moduli from deflection data was accomplished by deploying MODULUS v.6, with pavement modeled as a four-layer system and, in a few cases, as a three-year system as well. The backcalculated results show that the moduli of all the sections, except that of the CFA, increased steadily from 28 days to 1654 days. In CFA, however, the modulus was not only relatively low but it also leveled off after 440 days. In the LFA section, the modulus remained significantly low in the beginning and continued at a low level over the five-year period. Unconfined compressive strength (UCS) determined from 102-mm (4-in.) diameter cores consistently increased with time in all of the six mixes. The strength gain of the 5.5% cement control mix leveled off after 440 days, thus not attaining the target strength of 2070 kPa (300 psi). Lime-fly ash mix strength was indeed low compared to those of the other mixes. With 220 mm (8.75 in.) of HMA overlay, no reflection cracks were observed throughout the five-year monitoring period.

For a comparative evaluation of the six sections, their short- and long-term performance was examined; short-term performance in terms of 28-day shrinkage cracks in the base layer and long-term performance in terms of stiffness modulus and UCS. Though considered satisfactory in regard to shrinkage cracks, the long-term performance of the LFA mix is suspect as evidenced by its low stiffness, and in turn, large deflection. Though structurally adequate, based on the questionable short-term performance of both the CFA and LGBFS mixtures, their use in flexible pavement beneath HMA, especially thin layers, (102 mm [4 in.] or less) is deferred. Mixing two additives in small proportions is another construction-related problem in the CFA and LGBFS mixtures. The control CTM with 5.5% cement not only suffered excessive shrinkage cracking, but also its long-term strength fell short of expectation. Although the precut CTM is structurally sound, two problems dissuade its application: excessive shrinkage cracking and the logistics of cutting grooves while the layer is being compacted. From the point of view of overall performance, precracked CTM indeed excelled beyond all of the other treatments/admixtures and therefore is recommended for stabilization of base layers.

REFERENCE

George, K.P., *Soil Stabilization Field Trial*, SN2581, Portland Cement Association, Skokie, Illinois, USA, 2006, 63 pages.

TABLE OF CONTENTS

1.	INTRODUCTION.....	1
1.1	Background.....	1
1.2	Scope/Objective of the Study.....	3
1.3	Scope of this Final Report.....	4
1.4	Summary.....	5
2.	FIELD TEST RESULTS.....	6
2.1	Project Description.....	6
2.2	Field Evaluation Tests.....	8
2.2.1	Falling Weight Deflectometer Study (December 1, 2004).....	8
2.2.2	Core Samples from Stabilized Layer (March 15, 2005).....	8
2.2.3	Dynamic Cone Penetration Tests (March 15, 2005).....	9
2.2.4	Crack Mapping (March 15, 2005).....	9
2.3	Summary.....	9
3.	RESULTS AND DISCUSSION.....	10
3.1	Introduction.....	10
3.2	FWD Deflection at the Plate Center.....	10
3.3	Modulus of Stabilized Layer.....	11
3.3.1	Sections 1A and 3A (Cement Control).....	13
3.3.2	Sections 1B and 3B (Precut).....	13
3.3.3	Section 2 (Precracked).....	13
3.3.4	Section 4 (Cement-Fly Ash).....	20
3.3.5	Section 5 (lime-GGBFS).....	25
3.3.6	Section 6 (Lime-Fly Ash).....	25
3.3.7	Section 6 (Alternate).....	28
3.4	Lime-Treated Subgrade.....	32
3.5	Hot Mix Asphalt Surface.....	35
3.6	Subgrade.....	37
3.7	Pavement Cores.....	37
3.7.1	Unconfined Compressive Strength (UCS).....	39
3.7.2	Unconfined Compressive Strength Comparison.....	41
3.7.3	Unconfined Compressive Strength Affected by Uneven Mixing.....	44
3.8	Dynamic Cone Penetration (DCP) Tests.....	44
3.9	Summary.....	48
4.	PRECRACKING DAMAGE INVESTIGATED EMPLOYING MODAL ANALYSIS.....	50
4.1	Introduction.....	50
4.2	Sample Preparation.....	51
4.3	Experimental Setup for Vibration Study.....	51
4.4	Verification of Modal Analysis Test Methodology.....	54
4.5	Animation of Mode Shapes Employing ME'Scope VES.....	54
4.6	Results and Discussion.....	54
4.7	Summary.....	56
5.	SUMMARY AND CONCLUSIONS.....	58
5.1	Shrinkage Cracks.....	58
5.2	Performance of Sections Based on Stiffness and Strength of Stabilized Soil.....	60

5.3	Overall Conclusions.....	61
5.4	Recommendations.....	63
	REFERENCES.....	65
	APPENDIX A.....	67
	APPENDIX B.....	68

LIST OF TABLES

3.1	Comparison of FWD Deflections (Center of 12-in. Plate). Normalized and Averaged Over the Section for 1564-day, 1034-day, and 440-day tests.....	11
3.2	Comparison of Backcalculated Moduli Computed from 28-day, 440-day, 1034-day, and 1564-day FWD Deflection Tests. Control Cement Section	14
3.3	Comparison of Backcalculated Moduli Computed from 28-day, 440-day, 1034-day, and 1564-day FWD Deflection Tests. Precut Cement Section.....	16
3.4	Comparison of Backcalculated Moduli Computed from 28-day, 440-day, 1034-day, and 1564-day FWD Deflection Tests. Precracked Cement Section.....	18
3.5	Comparison of Backcalculated Moduli Computed from 28-day, 440-day, 1034-day, and 1564-day FWD Deflection Tests. Cement-Fly Ash Section.....	21
3.6	Comparison of Backcalculated Moduli Computed from 28-day, 440-day, 1034-day, and 1564-day FWD Deflection Tests. Lime-GGBFS Section.....	22
3.7	Comparison of Backcalculated Moduli Computed from 28-day, 440-day, 1034-day, and 1564-day FWD Deflection Tests. Lime-Fly Ash Section Without Drainage Layer.....	23
3.7.a	Moduli Computed from 1034-day and 1564-day FWD Deflection Tests. Lime-Fly Ash Section Without Drainage Layer. Three-layer Analysis.....	29
3.8	Comparison of Backcalculated Moduli Computed from 28-day, 440-day, 1034-day, and 1564-day FWD Deflection Tests. Lime-Fly Ash Section with Drainage Layer. LFA and Lime-treated Subgrade Combined.....	30
3.9	Composite Modulus Comparison Between Sections 6 and 6 (Alternate) of 1564-day and 1034-day FWD Deflection Tests.....	31
3.10	Thickness of HMA and Core Samples, and Classification of the Latter.....	40
3.11	Properties of Core Samples and Unconfined Compressive Strength at 1564 days, corrected to 2:1 height-to-diameter ratio.....	42
3.12	Dynamic Cone Penetration (DCP) Test Results. Unconfined Compressive Strength (UCS) of Lime-treated Subgrade and Resilient Modulus (M_R) of Subgrade from Respective DCP Indices.....	47
5.1	Short-term and Long-term Performance Compared and Rated.....	60

LIST OF FIGURES

2.1	Typical cross section of test sections, Mississippi Highway #302, Marshall County.....	7
3.1	Modulus (backcalculated) increase with time of the control section. E_2 = Modulus of cement stabilized layer, E_3 = Modulus of lime-treated subgrade, E_4 = Modulus of subgrade.....	15
3.2	Modulus (backcalculated) increase with time of the precut section. E_2 = Modulus of cement stabilized layer, E_3 = Modulus of lime-treated subgrade, E_4 = Modulus of subgrade.....	17
3.3	Modulus (backcalculated) increase with time of the precracked section. E_2 = Modulus of cement stabilized layer, E_3 = Modulus of lime-treated subgrade, E_4 = Modulus of subgrade.....	19
3.4	Modulus (backcalculated) increase with time of the cement-fly ash section. E_2 = Modulus of cement-fly ash soil, E_3 = Modulus of lime-treated subgrade, E_4 = Modulus of subgrade.....	24
3.5	Modulus (backcalculated) increase with time of the lime-GGBFS section. E_2 = Modulus of lime-GGBFS soil, E_3 = Modulus of lime-treated subgrade, E_4 = Modulus of subgrade.....	26
3.6	Modulus (backcalculated) change with time of the lime-fly ash section without drainage layer. E_2 = Modulus of lime-fly ash soil, E_3 = Modulus of lime-treated subgrade, E_4 = Modulus of subgrade.....	27
3.7	Modulus (backcalculated) variation of lime-treated subgrade, E_3 , along the road.....	33
3.8	Modulus (backcalculated) variation of lime-treated subgrade, E_3 (section average).....	34
3.9	Modulus (backcalculated) variation of hot-mix asphalt, E_1 (section average). (7 refers to section 6 [alternate].).....	36
3.10	Modulus (backcalculated) variation of subgrade, E_4 (section average). (7 refers to section 6 [alternate].).....	38
3.11	DCP test results in section 1B, Hwy #302, Marshall County.....	46
3.12	DCP test results in section 4, Hwy #302, Marshall County.....	46
4.1	Modulus before and after precracking (adapted from reference 14).....	51
4.2	Schematic of the experimental setup (adapted from reference 19).....	52

4.3	Typical frequency response function (adapted from reference 19).....	53
4.4	Healing in material with curing time. Damage is the ratio of loss in stiffness of precracked beam to the stiffness of control beam (adapted from reference 19).....	55
5.1	Evolution of crack density with time (adapted from reference 14).....	59

CHAPTER 1

INTRODUCTION

1.1 Background

Stabilizing agents such as cement, lime, lime-fly ash, and others have been used successfully in pavement base/subbase construction. There is concern, however, over possible shrinkage cracking due to shrinkage and/or thermal contraction, especially in high-strength cement-stabilized soil. Shrinkage, especially early shrinkage and consequent cracking, has been a concern for pavement engineers. Shrinkage of cement-treated materials (CTM) can be divided into two categories: autogeneous shrinkage (shrinkage resulting from the hydration of the cement) and drying shrinkage. Though drying causes the majority of the shrinkage (George 1968 and Bofinger, Hassan, Williams 1978), other factors also contribute to shrinkage: amount and type of clay in the treated material, pretreatment and molding moisture content, and cement content, to name a few (George 1968 and Bofinger, Hassan, Williams 1978). While cement content historically is believed to influence shrinkage, a recent study noted an optimal cement content existed where total shrinkage was minimized (George 1968 and Scullion, Sebesta, Harris, Syed 2000). With the developed understanding of the factors causing shrinkage in CTM, recent efforts for minimizing the shrinkage cracking problem focused on mix design and construction aspects of the CTM layer. The Portland Cement Association currently recommends 7-day unconfined compressive strengths in the range of 2070-2760 kPa (300-400 psi) in the design phase, and during construction compaction at or slightly below optimum moisture content, and moist curing until a moist barrier is placed (PCA 2003). Other studies suggest that shrinkage cracking can be abated by adopting materials and/or methods that bring about a “desirable” crack pattern, “desirable” being defined as numerous fine cracks at close spacing, which ensures adequate load transfer across the cracks. It is not so much the number of cracks but the width of these cracks that has a significant influence on the long-term performance of the pavement, since wider cracks have the tendency to reflect through the overlying pavement. Limiting/controlling drying shrinkage can effect the development of this “desirable” crack pattern in a stabilized layer. Several alternatives are available to control the drying shrinkage. These include: judiciously selecting the cement dosage, selecting a soil for stabilization having limited fines content and plasticity, and the use of lime-fly ash additive, all of which promote development of a “desirable” crack pattern in a stabilized layer.

Controlling shrinkage cracks, even before they begin to crop up, is another method to alleviate the detrimental affects of this cracking in pavement performance. This control can be effected by “precutting” to induce a weak plane in the stabilized layer or “precracking” at an early age (from 24 to 72 hours after construction) by three to four passes of a vibratory roller with 100% coverage.

Originally introduced in France (Colombier and Marchand 1996), the underlying principle of precutting is that by introducing grooves/cuts at close intervals (for instance, 3m apart) crack width can be controlled. Viewed differently, this technique is intended to prevent the occurrence of occasional but relatively wide and damaging natural cracks which can easily propagate through bituminous surfacing due to relative vertical movement of the crack edges under trafficking, therefore necessitating thick bituminous surfacing. Benefits of precutting are described in other studies (Shahid, Thom 1996 and Lefort 1996). Precracking has been a subject

of experiments in the past in cement-treated pavement bases. The basic premise of this technique is that by precracking (with a vibratory roller), “young” cement base experiences numerous fine or hairline cracks at close spacing. The success of this method depends on inducing cracks while the cement hydration is in progress. The first reported successful experiment of precracking by immediate traffic release was conducted in Japan, with encouraging results (Yamanouchi and Ihido 1982). An experimental section built in Mississippi (Teng and Fulton 1974), where the road was opened to traffic immediately, has performed better than a control section where traffic was redirected for a minimum of 7 days. Even more encouraging results are reported from Austria (Litzka and Haslehner 1995), where the cement base was subjected to several passes of a 12-ton vibratory roller between 24 and 72 hours after construction. A comparison between deflection measurements before and after microcrack initiation showed an increase of the mean values, from 1.09 mm to 1.32 mm. Nevertheless, this increase of deflection is reduced in the course of the setting process, suggesting healing of cracks. Brandl (Brandl 1999) reported that, of the available options for minimizing cracking on the Austrian-Hungarian Highway, the microcracking technique was most suitable. In August 2000 MDOT sponsored a research project in which precracking technique was successfully implemented; the results of this study will be presented in the latter sections of this report. The second trial in the United States was carried out at the Texas Transportation Institute, TTI (Scullion and Saaverketo 2002). Three test sections were built in late 2000 and overlaid with 50 mm (2 in.) hot mix asphalt (HMA). Six-month monitoring results showed that (i) the precracked base was very stiff and (ii) only a minor amount of cracking was found in each section. Another follow-up study at TTI (Sebesta 2005) with no HMA overlay confirmed the earlier results, i.e., precracking (microcracking) proved quite effective at reducing shrinkage cracking problems in the base. It was also reported that microcracking did not result in pavement damage or diminished in-service modulus.

1.2 Scope/Objective of the Study

Seeking materials and methods to alleviate cracking in cement-treated soil, six field sections were constructed on August 17 and 18, 2000, incorporating the following material combinations or methods each in a separate but contiguous test section 305 m (1000 ft) long: cement, precracked cement layer, precut cement layer, cement-fly ash, lime-ground granulated blast furnace slag (GGBFS), and lime-fly ash (LFA). The special procedures of precracking and precutting were intended, respectively, to minimize the detrimental effects of shrinkage cracks by forcing them to spread evenly (that is, promoting microcracks), and to facilitate cracks cropping up in the precut grooves. The stabilizing additives were selected judiciously to accomplish low-strength stabilized soil and also to restrain the rate of strength gain, especially during the early period.

1.3 Scope of this Final Report

The first interim report covering the mix design procedures, construction details, construction control tests, and first phase of investigation/monitoring during the 28-day period was submitted April 21, 2001 (George 2001). Two layers of asphalt concrete – 110-mm (4.5-in.) base, 60-mm (2.25-in.) polymer modified binder – were placed over the stabilized layer beginning September 21, 2000, followed by the second field monitoring on November 13, 2001. Field tests included deflection tests employing Falling Weight Deflectometer (FWD), retrieval of 100-mm (4-in.)

cores for compression tests, and a manual crack survey. The results were presented in Interim Report II (George 2002), which included a discussion of possible changes (strength- and stiffness-gain, and crack reflection) over the 14-month period since September 15, 2000, when the first monitoring was completed. On June 16, 2003 (nominally 3 years), the test sections were monitored, again using deflection tests employing FWD and a manual crack survey. Prior to the June 2003 survey, a 50-mm (2-in.) polymer modified surface course was placed, with the road opening to traffic on July 8, 2002. Presented in Interim Report III (George 2003) were the results of deflection analysis discussing comparative performance of various stabilizing agents or special crack mitigation techniques included in the test program. The fifth year deflection testing employing FWD was completed on December 1, 2004, and stabilized soil cores for compression tests were retrieved on March 8, 2005. Following the retrieval of hot mix asphalt and stabilized base cores, the underlying lime-treated layer and subgrade were tested with Dynamic Cone Penetrometer (DCP) to determine the thickness of the former layer and stiffness modulus of the subgrade layer. A crack survey was conducted as well. This Final Report presents the following: (i) results of deflection analysis and moduli of layers, (ii) compressive strength results of 100-mm (4-in.) diameter cores, (iii) DCP test results and moduli of subgrade layer calculated from them, and (iv) the crack survey results. Comparative performance of various stabilizing agents and special techniques in mitigating cracks are discussed, delineating promising additives/techniques for stabilization application.

1.4 Summary

This chapter lists the tests conducted on the six-section test project, followed by a brief review of recent developments in the area of mitigating shrinkage cracks in stabilized soil (for pavement construction). The field investigation includes FWD tests, coring of stabilized layers for unconfined compression testing and DCP tests in the core holes investigating the lime-treated subgrade and underlying subgrade. A manual crack survey completes the final phase of the investigation.

CHAPTER 2

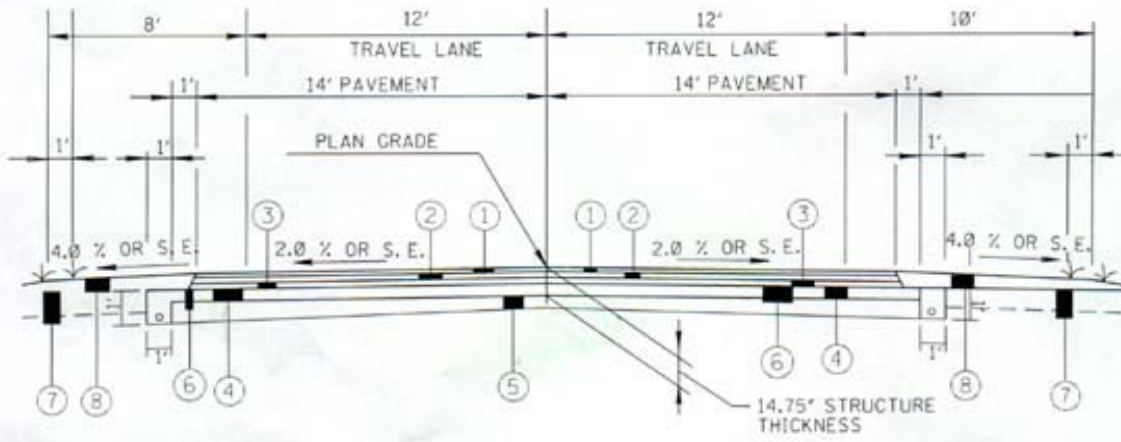
FIELD TEST RESULTS

2.1 Project Description

Six test sections were included in the westbound lane of Highway #302 in Marshall County, Mississippi. Each test section was 305 m (1000 ft) long and 8.5 m (28 ft) wide, though only the traffic lane 4.25 m (14 ft) wide was tested. A typical cross section of the test pavement is presented in Figure 2.1, where the 1524-m (5000-ft) LFA base was replaced by five other stabilized layers, 305 m (1000 ft) each. With an MDOT standard LFA base 305 m (1000 ft) at the east end included in the test program for comparison purposes, the field trial comprises the following six additives/procedures:

- 190+00 to 195+00: cement 5.5%, cement control – Section 1A
- 195+00 to 200+00: cement 5.5%, precut – Section 1B
- 200+00 to 210+00: cement 5.5%, precracked – Section 2
- 210+00 to 215+00: cement 5.5%, cement control – Section 3A
- 215+00 to 220+00: cement 5.5%, precut – Section 3B
- 220+00 to 230+00: cement 3.5% and fly ash 8% (CFA) – Section 4
- 230+00 to 240+00: lime 2% and GGBFS 6% (LGBFS) – Section 5
- 245+00 to 250+00: lime 3% and fly ash 12% (LFA), MDOT Standard – Section 6
- 250+00 to 255+00: lime 3% and fly ash 12% with 10-cm (4-inch) drainage layer – Section 6 (alternate)

In order to eliminate unforeseen variations while transitioning from one section to another, each end of a test section – 31 m (100 ft) in 305-m-(1000-ft-) long sections and 15 m (50 ft) in 152-m-(500-ft-) sections – was not monitored, leaving three 244-m-(800-ft-) test sections and six 122-m-(400-ft-) sections.



TYPICAL SECTION

- ① 2" HOT MIX ASPHALT, HT, POLYMER MODIFIED REQ'D. [1 @ 2" (12.5 mm MIXTURE)].
 - ② 2.25" HOT MIX ASPHALT, HT, POLYMER MODIFIED REQ'D. [1 @ 2.25" (19 mm MIXTURE)].
 - ③ 4.5" HOT MIX ASPHALT, HT, REQ'D. [2 @ 2.25" (19 mm MIXTURE)].
 - ④ 6" LIME-FLY ASH BASE COURSE REQ'D. (INCORPORATED 3% LIME AND 12% FLY ASH INTO CL. 9, GROUP C, GRANULAR MATERIAL TO PRODUCE 6" COMPACTED LIME-FLY ASH COURSE(30' WIDE)).
 - ⑤ 6" CHEMICALLY TREATED SUBGRADE REQ'D. LIME TREATED (4% LIME).
 - ⑥ 6" GRANULAR MATERIAL (CL. 9, GP. C) REQ'D. *SEE NOTE.
 - ⑦ 12" & VAR. GRANULAR MATERIAL (CL. 9, GP. C) REQ'D.
 - ⑧ 8.75" & VAR. GRANULAR MATERIAL (CL. 3, GP. D) REQ'D.
- * THE DESIGN SOIL WAS GRADED TO 2% CROSS SLOPE 15' LT. & RT. OF CENTER LINE THROUGHOUT PROJECT.

Figure 2.1 Typical cross section of test sections, Mississippi Highway #302, Marshall County.

2.2 Field Evaluation Tests

2.2.1 Falling weight deflectometer study (December 1, 2004). Assisted by the MDOT Research Division, deflection measurements were conducted on the HMA every 31 m (100 ft) along each test section, thus gathering nine deflection test data in each 1000-ft-section and five in each 500-ft-section. The following test setup was used: three seating drops followed by 71-kN- (16,000-lb-) and 76-kN (17,000-lb-) load drops at each test location. For brevity, FWD deflection data will not be included in this report; however, the backcalculated modulus of each test section is reported and discussed in Chapter 3.

2.2.2 Core samples from stabilized layer (March 15, 2005). Three 100-mm-(4-in.-) diameter stabilized material cores from 244-m-(800-ft-) sections and two from 122 m (400 ft) were extracted. In order to reach the stabilized layer, the HMA layer was cored as well, measuring precisely the thickness of the asphalt and stabilized layers which were employed in the backcalculation routine.

The stabilized layer cores were wiped dry, wrapped, and brought to the laboratory. The cores were capped with plaster of paris, as required, and tested for compressive strength in accordance with ASTM D 1633-84. With core samples having different heights, the strengths of each sample were corrected to correspond to height to diameter ratio of 2:1.

In all of the sections (except in the LFA) the cores remained intact whereas the LFA cores were eroded by the diamond drill grinding away sand particles. As a result of excessive grinding, the LFA samples were undersize, diameter about 96 mm (3.8 in.) in contrast to 100 mm (4 in.), nominal diameter of the core bit. The drilling in section 6 (alternate) was unsuccessful because the cores completely disintegrated due to being ground by the stone chips from the drainage layer overlying the LFA base.

2.2.3 Dynamic cone penetration tests (March 15, 2005). In order to determine the thickness of the subbase layer, which serves as an input in the backcalculation analysis, Dynamic Cone Penetrometer tests were conducted in the core holes for a depth in excess of 500 mm after removing the stabilized base core. Both treated subgrade and the subgrade layer were tested in each hole.

2.2.4 Crack mapping (March 15, 2005). Following the classification adopted in the First Interim Report (fine, low, medium, high severities) (14), a crack survey was conducted. The HMA surface was completely crack-free, as expected.

2.3 Summary

A complete description of the project is presented, detailing the additive content of each section and/or procedures implemented with the objective of mitigating shrinkage cracks. Brief descriptions of each field test and data analysis procedure comprise the latter part of this chapter.

CHAPTER 3

RESULTS AND DISCUSSION

3.1 Introduction

The purpose of the five-year investigation is to discern whether the stabilized layer has improved in stiffness as a result of continued pozzolonic reaction producing cementitious compounds. But for a short period of 7 to 28 days, the stabilized layer continued to gain strength. The severe hot temperature that existed during and after construction could have caused this temporary setback in the strength gain. From 28 days to 440 days (11/13/2001), however, all six stabilized bases improved so far as the modulus is concerned. Beyond 440 days, with the road opening to traffic on 5/6/2002, the stiffness modulus of five sections increased, whereas in the CFA section it remained practically unchanged. The issue addressed here is whether the stabilized layers continue to gain stiffness and strength after the road is trafficked for nearly 2 ½ years.

3.2 FWD Deflection at the Plate Center

For a direct comparison of the structural adequacy of the six test sections, the first sensor deflection at three periods over a three-year window is normalized with respect to the load, and listed in Table 3.1. At the outset, it should be remarked that at 440 days, the pavement had received only 171 mm (6.75 in.) of HMA compared to 222 mm (8.75 in.) while being FWD-tested at 1034 days, possibly one reason for the 440-day deflection being relatively large. The fact that the 440-day and 1564-day tests were conducted during cold weather (average air temperature of 60° F), however, had an opposite effect on the deflection response. Note that the average air temperature during the 1034-day test was 90° F. More or less, it is the same temperature effect – warm weather at 1034 days and cold weather at 1564 days – that suppressed the 1564-day deflection in comparison to the earlier test at 1034 days.

Table 3.1 Comparison of FWD Deflections (Center of 12-in. Plate). Normalized and Averaged over the Section for 1564-day, 1034-da, and 440-day Tests

Section No.	1564-day (12/01/2005) deflection, in./lb(E-07)	1034-day (6/16/2003) deflection, in./lb(E-07)	440-day (11/13/2001) deflection, in./lb(E-07)
1A & 3A	3.95	5.04	4.47
1B & 3B	4.21	5.09	4.96
2	3.52	5.23	4.64
4	4.05	5.24	5.06
5	3.48	4.86	5.05
6	5.65	8.86	8.11

One noteworthy observation from a comparison of the section deflections is that the LFA section deflection is consistently approximately 60% larger, a clear indication of its structural inadequacy. The UCS and backcalculated modulus results substantiate this premise in that all of the pavement layers in the LFA section appeared relatively weak as judged by the backcalculated moduli. Not only the LFA modulus but also those of other layers – HMA, lime-treated subgrade, and even the subgrade – seem to have been negatively impacted by the inherent weakness of the LFA layer.

3.3 Modulus of Stabilized Layer

Employing the deflection bowl obtained from FWD tests, moduli of the layers were backfigured. Backcalculation program MODULUS v.6 and ELMOD were utilized, with the pavement modeled as a four-layer system. Pavement layer thicknesses are appropriately modified from design values reflecting those measured during coring of samples. Whenever the results were inconclusive, a three-layer analysis (with stabilized base and lime-treated subgrade clubbed together) was conducted to substantiate the four-layer analysis. Section #6 alternate of the LFA Section (Station 250+00 to 255+00) included a 10-cm (4-in.) drainage layer as well where, by necessity, the stabilized layer and the lime-treated subgrade combined to form a 30-cm (12-in.) composite layer. Combining those two layers could be justified in view of close modulus values of LFA and lime-treated material.

The moduli results of 1564-day deflection studies are compared with those of the 1034-day, 440-day, and 28-day FWD tests (see Tables 3.2 through 3.8). The modulus of the asphalt layer is corrected to 22° C (72° F) temperature, in accordance with the BELLS3 method described in reference 17. In computing the average for each test section, outliers are detected by Chauvenet's criterion.

The 1034-day deflection basins of the first three sections (control, precut, and precrack) were reanalyzed with slightly revised Poisson's ratio for stabilized cement layer, and though results are entered in Tables 3.2 through 3.4. The revised Poisson's ratio is 0.30 in contrast to 0.25 employed in the Interim Report III. The 1034-day moduli values reported for the three sections in this report are slightly different, which could be attributed to the small increase in Poisson's ratio (0.25 to 0.30), and also to the use of an advanced version of MODULUS program, namely version 6.

A brief discussion of the modulus of the stabilized layers is presented in two parts: first, how much increase is observed from 1034 to 1564 days, and second, a comparison of the four experimental sections with the cement control section followed by another comparison of LFA base with cement control section.

3.3.1 Section 1A and 3A (cement control). In this section the 1564-day modulus of stabilized layer increased by 46% from the 1034-day modulus, whereas the net gain from 28 to 1564 days was 68% (Table 3.2). Clearly the stiffness gain of the stabilized layer was reversed from 440 to 1034 days, a very unlikely event. The problem of "compensating effect" arising in backcalculation procedure could be a reason for this anomalous result. Perhaps attributable to the deflection bowl, the backcalculated modulus of one layer increases with the corresponding decrease in the modulus of the adjacent layer, which is referred to as compensating effect. The modulus of the treated subgrade increased steadily (320 MPa to 1900 MPa) in the five-year period, however (Figure 3.1). The same trend, i.e., an approximately four-fold increase in the modulus of lime-treated subgrade, was observed in other treated subgrade sections as well, especially in precut and precracked sections.

3.3.2 Sections 1B and 3B (precut). The modulus after 1564 days was 16% larger compared to that of 1034 days (Table 3.3 and Figure 3.2). Initially, due to the precuts, the 28-day and 440-day modulus lagged behind that of the control section. However, at 1034 days the modulus had caught up with that of the control section, showing nearly identical moduli. The net gain in stiffness over the five-year period was 53%, slightly exceeding the 46% increase in the control section.

3.3.3 Section 2 (precracked). The stabilized layer modulus at 1564 days was 15% larger than the 1034-day modulus (Table 3.4). It is observed that the cement stabilized layer gained its stiffness at a faster rate from 28 to 440 days (57%) when compared to the gain from 440 to 1034 days (13%) (Figure 3.3). However, the 1034-day modulus of 2450 MPa is comparable to that of the control section. Note that all of the cement sections gained stiffness attaining nearly identical values, respectively, 3100 MPa, 3150 MPa, and 2820 MPa for control, precut, and precracked sections.

**Table 3.2 Comparison of Backcalculated Moduli Computed from 28-day, 440-day, 1034-day, and 1564-day FWD Deflection Tests
Control Cement Section**

Section	Station	1564 - day Modulus, MPa ^a				1034 - day Modulus, MPa ^a				440 - day Modulus, MPa ^a				28 - day Modulus, MPa ^a			
		E1	E2	E3	E4	E1	E2	E3	E4	E1	E2	E3	E4	E1	E2	E3	E4
1-A	190+50	8469	4917	2041	138					6760	4780	890	160	—	2540	210	80
	191+50	7552	3834	1352	131	9679	2990	1559	152	8540	2320	660	140	—	1380	260	90
	192+50	7618	4634	3090	145	9769	3158	1738	145	6590	2110	750	250 ^b	—	190 ^d	730 ^d	120 ^b
	193+50	6800	1690	1648	124	9261	2426	797	150	7090	2300	490	110	—	1450	1310 ^b	90
	194+50					12627	757	703	111	9970	850	390	100	—	810 ^c	380 ^c	80 ^c
3-A	210+50	9138	1497	1241	159	7566	3252	610	160	10520	2940	440	180	—	1160	200	80
	211+50	6862	745	3138	152	9080	1070	675	163	7500	1680	570	180	—	980	230	90
	212+50	12531	4255	1380	172	11582	3100	2034	172	7900	2460	1030 ^b	210	—	3270	100	70
	213+50					12174	2960	2926	123	15310 ^b	4730	650	150	—	2570	740	80
	214+50	12097	3262	1317	138	9709	1701	1699	149	12110	2960	550	160	—	1430	520	100
	Mean CoV	8420 25.4	3100 51.2	1900 41.6	150 10.8	10160 16.1	2230 40.4	1570 55.6	150 13.1	8550 22.4	2710 45.5	600 26.3	150 22.5	—	1850 44.8	320 69.6	90 10.9

^a 1 MPa = 0.145 ksi

^b Outlier tested according to Chauvenet's criterion

^c Not considered in the average calculation because of unsatisfactory deflection bowl

E1 Modulus of HMA

E2 Modulus of cement-treated soil

E3 Modulus of lime-treated subgrade

E4 Modulus of subgrade

CoV Coefficient of variation (%)

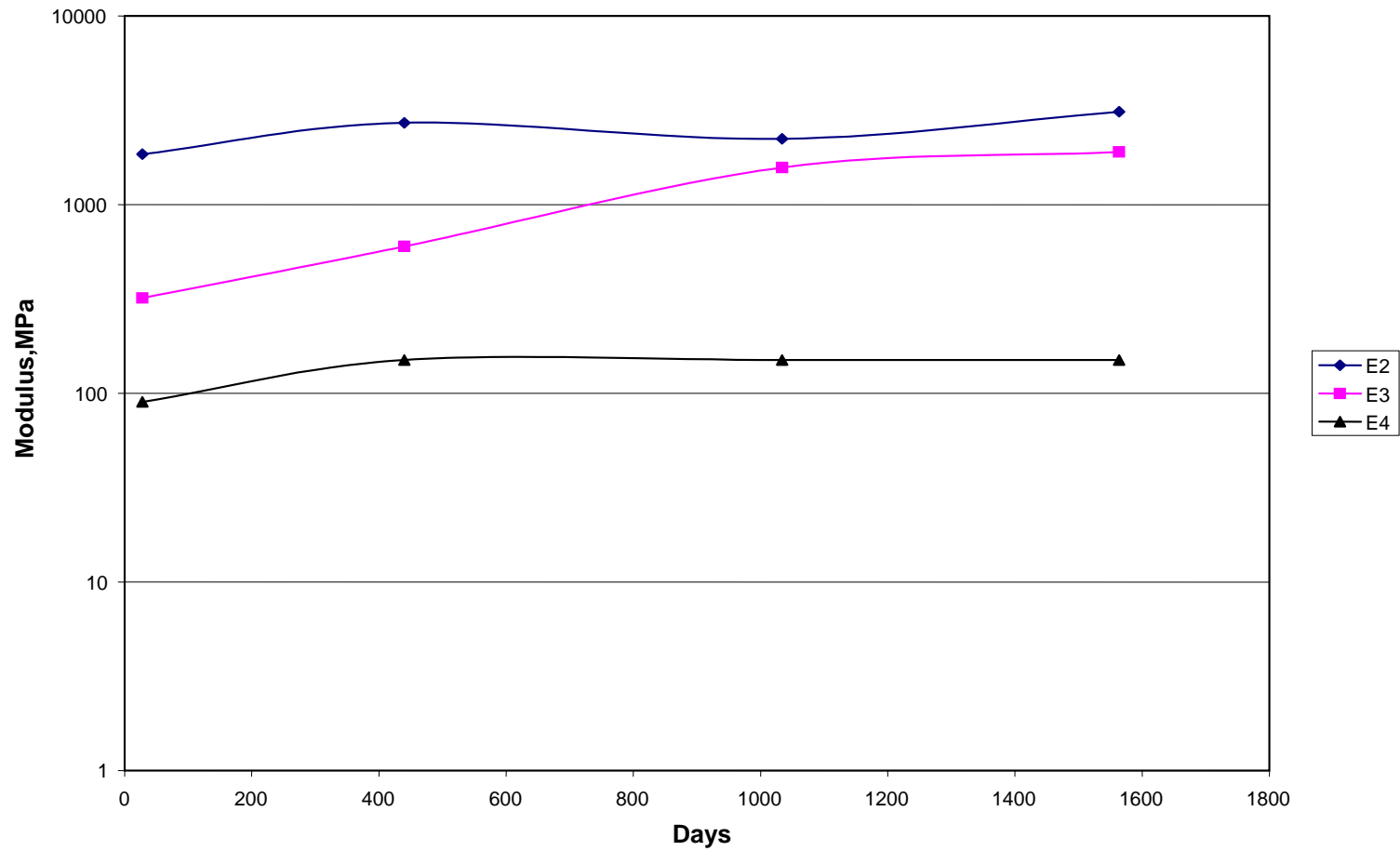


Figure 3.1 Modulus (backcalculated) increase with time of the control section. E_2 = Modulus of cement stabilized layer, E_3 = Modulus of lime-treated subgrade, E_4 = Modulus of subgrade.

Table 3.3 Comparison of Backcalculated Moduli Computed from 28-day, 440-day, 1034-day, and 1564-day FWD Deflection Tests Precut Cement Section

Section	Station	1564 - day Modulus, MPa ^a				1034 - day Modulus, MPa ^a				440 - day Modulus, MPa ^a				28 - day Modulus, MPa ^a			
		E1	E2	E3	E4	E1	E2	E3	E4	E1	E2	E3	E4	E1	E2	E3	E4
1-B	195+50									13250	1150	470	90	—	940	770	90
	196+50	8945	2131	1938	124	11918	2394	1523	143	6990	3010	710	140	—	1340	890	130
	197+50	10359	2841	772	97	12527	2261	1890	103	7950	2070	380	120	—	2670	520	110
	198+50	6269	5138	1559	131	12280	5786 ^b	1143	147	12990	2240	480	120	—	1660	170	160
	199+50	6117	5834	1255	131	10443	2588	1537	137	10640	2210	420	100	—	600 ^c	210 ^c	160 ^c
3-B	215+50	7476	1117	3386 ^b	117	10574	1593	1366	145	7700	1810	840	140	—	1500	440	110
	216+50	7800	972	1000	117												
	217+50	8400	1559	1483	221 ^b					8720	2810	360	170	—	3430 ^b	610	140
	218+50	8117	2524	2352	138	9407	3828	1529	158	9830	3440	760	170	—	1060	320	110
	219+50	8014	6186	2400	159	9790	3629	1396	194	9420	9580 ^b	210 ^b	200	—	1520	190	140
	Mean	7950	3150	1590	120	10990	2720	1480	150	9560	2240	530	140	—	1470	540	120
	CoV	16.3	64.9	37.5	14.3	11.3	31.5	15.3	18.4	22.9	30.9	34.0	25.8		37.1	53.4	18.3

^a 1 MPa = 0.145 ksi

^b Outlier tested according to Chauvenet's criterion

^c Not considered in the average calculation because of unsatisfactory deflection bowl

E1 Modulus of HMA

E2 Modulus of precut cement-treated soil

E3 Modulus of lime-treated subgrade

E4 Modulus of subgrade

CoV Coefficient of variation (%)

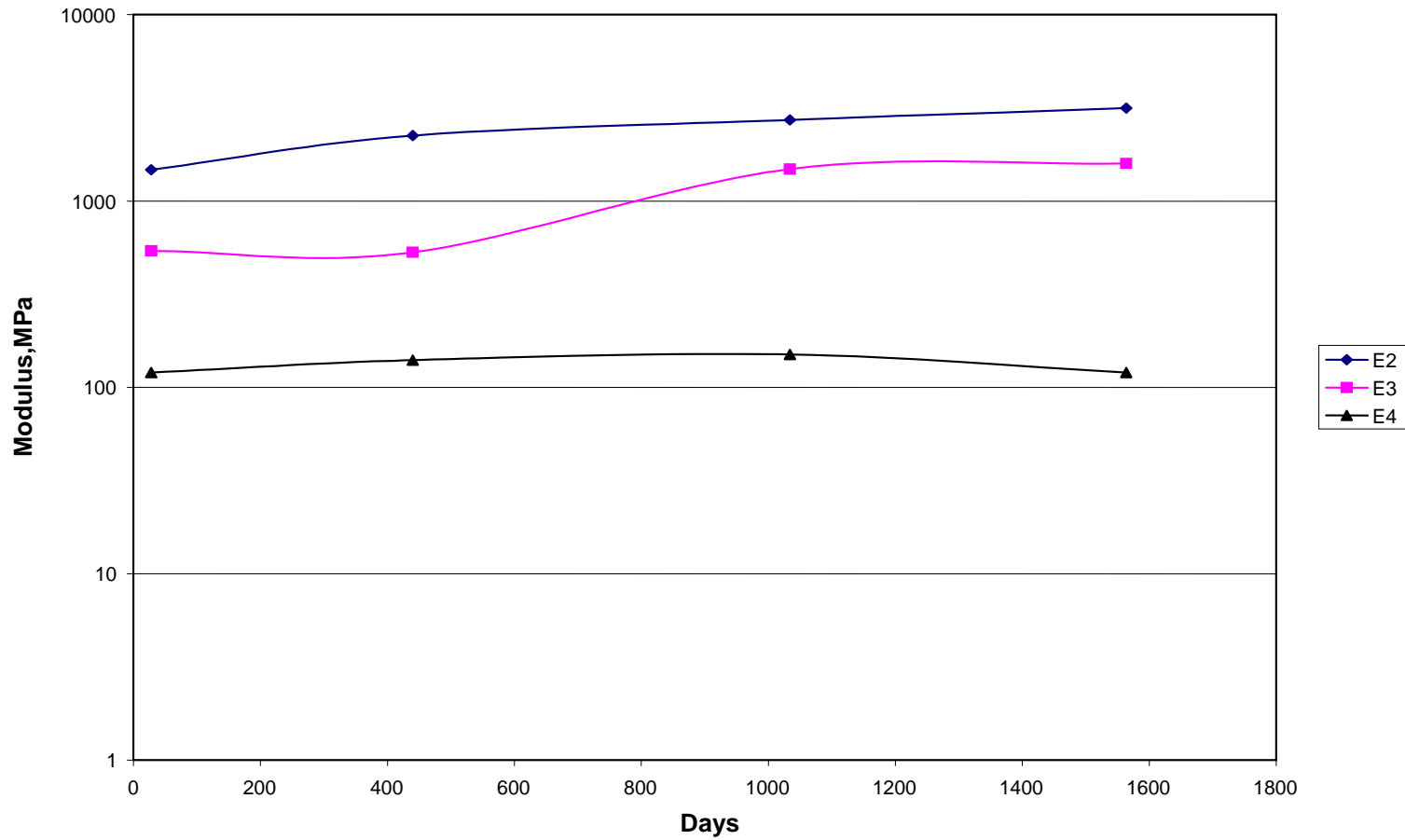


Figure 3.2 Modulus (backcalculated) increase with time of the precut section. E_2 = Modulus of cement stabilized layer, E_3 = Modulus of lime-treated subgrade, E_4 = Modulus of subgrade.

Table 3.4 Comparison of Backcalculated Moduli Computed from 28-day, 440-day, 1034-day, and 1564-day FWD Deflection Tests Precracked Cement Section

Section	Station	1564 - day Modulus, MPa ^a				1034 - day Modulus, MPa ^a				440 - day Modulus, MPa ^a				28 - day Modulus, MPa ^a			
		E1	E2	E3	E4	E1	E2	E3	E4	E1	E2	E3	E4	E1	E2	E3	E4
2	201+00	9717	4538	455	152	12032	2621	1620	154	8580	2660	870	140	—	710 ^d	1430 ^d	140
	202+00	10372	3807	2717	193	11390	4622	2016	227								
	203+00	10228	3110	1779	221 ^b					12940	2990	450	150	—	2160	460	170
	204+00	11221	2834	2283	138	11298	3054	2024	138	13070	2540	620	150	—	290 ^d	1870 ^d	80
	205+00	7959	3979	1297	131	8472	1969	1052	130	8930	3010	860	110	—	720 ^d	940 ^d	80
	206+00	6876	1752	1607	124	10071	943	699	132	6930	1250	560	130	—	480 ^d	1800 ^d	90
	207+00	8669	924	2621	117												
	208+00	8372	2945	352	110	8069	1503	1034	110	8730	1240	490	140	—	990	590	90
	209+00	8048	1490	448	138					8050	1060	480	120	—	1950	320	70
	Mean	9050	2820	1500	140	10220	2450	1410	150	9280	2170	640	140	—	1380	410	100
	CoV	15.5	43.2	62.1	18.8	16.1	53.2	39.7	27.6	25.1	41.9	28.7	11.3		36.7	29.6	36.3

^a 1 MPa = 0.145 ksi

^b Outlier tested according to Chauvenet's criterion

^c Not considered in the average calculation because of unsatisfactory deflection bowl

E1 Modulus of HMA

E2 Modulus of precracked cement-treated soil

E3 Modulus of lime-treated subgrade

E4 Modulus of subgrade

CoV Coefficient of variation (%)

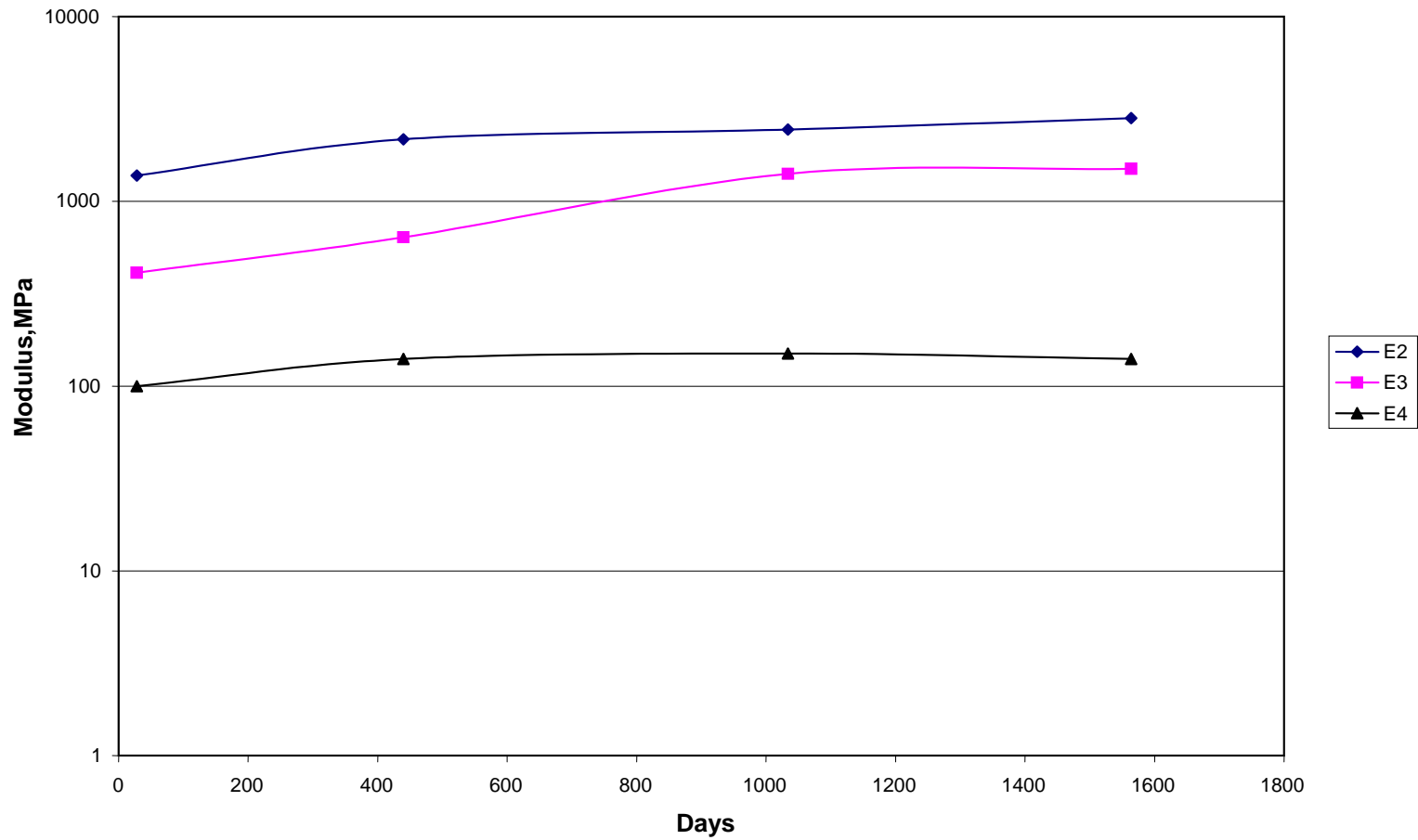


Figure 3.3 Modulus (backcalculated) increase with time of the precracked section. E_2 = Modulus of cement stabilized layer, E_3 = Modulus of lime-treated subgrade, E_4 = Modulus of subgrade.

3.3.4 Section 4 (cement-fly ash). The relatively large deflections observed in this section at 1034 days were repeated at 1564 days as well. After several unsuccessful trials with the MODULUS v.5.1 program, several other routines were experimented with, including MODULUS v.6, ELMOD, and EVERCALC. The results with EVERCALC were unsatisfactory, therefore its use was discontinued. As MODULUS v.6 was successful in the first three sections, it was deployed in cement-fly ash section data to note that the base modulus was lower than that of the treated (lime) subgrade (870 MPa vs. 3120 MPa). Not convinced by the modulus trend, the ELMOD program was employed for backcalculation of both 1034-day and 1564-day data. The results obtained from the “radius of curvature” option of the ELMOD program did not solve the modulus “reversal” issue. By a trial and error procedure, a specific methodology has been developed, resorting to the “deflection basin fit” option in ELMOD. A brief description of this methodology can be seen in Appendix A.

At the outset, it should be mentioned that both 1034-day and 1564-day deflections of the last three sections—cement-fly ash, lime-GGBFS and lime-fly ash—were analyzed employing ELMOD, whereas the earlier results (440-day, 28-day, and 7-day) by MODULUS 5.1. As can be seen in Tables 3.5, 3.6, and 3.7, the moduli “reversal” issue was resolved in cement-fly ash and lime-GGBFS sections when backcalculation was performed with ELMOD. This problem persisted in the LFA section, however.

Beyond 440 days, the CFA modulus decreased and then again increased, however, in 1564 days only the level of stiffness measured at 440 days (Figure 3.4) was attained. It could be that the CFA modulus reached its peak modulus in less than two years and leveled off beyond that time. When taking into account the low stiffness modulus value of lime-treated subgrade (215 MPa), the 2380 MPa modulus of CFA at 28 days is considered an over-prediction, a typical case of “modulus compensation” among two adjacent layers. Moduli at later stages -, 440 days, 1034 days, and 1564 days - are clearly lower than those of the cement control, indicating some deficiency in the CFA mix. As will be discussed in a latter section, this problem is attributed to not being able to attain a uniform mix with two additives (3.5% cement and 8% fly ash).

**Table 3.5 Comparison of Backcalculated Moduli Computed from 28-day, 440-day, 1034-day, and 1564-day FWD Deflection Tests
Cement-fly Ash Section**

Section	Station	1564 - day Modulus, MPa ^a				1034 - day Modulus, MPa ^a				440 - day Modulus, MPa ^a				28 - day Modulus, MPa ^a			
		E1	E2	E3	E4	E1	E2	E3	E4	E1	E2	E3	E4	E1	E2	E3	E4
4	222+00	7083	1228	1255	166	8572	1331	1303	159	6310	1450	630	140	—	434 ^d	2180 ^d	80
	223+00	8255	1214	572	179	10297	400	1331	138	8190	1450	280	140	—	330 ^d	2110 ^d	80
	224+00	6545	6076 ^b	1166	179	8993	3324 ^b	1848	152	7560	1510	1360 ^b	150	—	2760	170	70
	225+00	7248	2166	1779	179	8145	1600	959	193	5230	1540	540	150	—	920 ^c	280 ^c	90 ^c
	226+00	9772	1841	841	166	9193	1131	945	145	5260	1690	290	170	—	480 ^c	140 ^c	100 ^c
	227+00					8117	876	793	179	4950	1460	570	150	—	810 ^c	250 ^c	100 ^c
	228+00	7062	869	3910 ^b	159	8476	1710	766	172	6960	360 ^d	1140 ^d	180	—	830 ^c	250 ^c	100 ^c
	229+00	4745	1683	1662	207	7490	862	1441	179	6560	1580	660	160	—	2340	510 ^b	130 ^b
	Mean	7240	1500	1210	180	8680	1130	1150	170	6380	1530	510	155	—	2380	215	70
	CoV	21.2	31.9	38.2	8.9	9.8	40.7	31.8	11.6	18.4	5.7	34.0	9.1		11.7	0	7.5

^a 1 MPa = 0.145 ksi

^b Outlier tested according to Chauvenet's criterion

^c Not considered in the average calculation because of unsatisfactory deflection bowl

E1 Modulus of HMA

E2 Modulus of cement-fly ash section

E3 Modulus of lime-treated subgrade

E4 Modulus of subgrade

CoV Coefficient of variation (%)

**Table 3.6 Comparison of Backcalculated Moduli Computed from 28-day, 440-day, 1034-day, and 1564-day FWD Deflection Tests
Lime-GGBFS Section**

Section	Station	1564 - day Modulus, MPa ^a				1034 - day Modulus, MPa ^a				440 - day Modulus, MPa ^a				28 - day Modulus, MPa ^a			
		E1	E2	E3	E4	E1	E2	E3	E4	E1	E2	E3	E4	E1	E2	E3	E4
5	231+00					9841	3848	2007	207	6860	2270	1340	130	—	6900	200	100
	232+00	7476	5290	2455	228	6752	2359	1614	172	5170	2800	1300	130	—	4530 ^c	40 ^c	110 ^c
	233+00	5848	6455 ^b	3566	242	8166	2717	1717	221	8360	2780	1430	160	—	9960 ^b	840 ^b	90
	234+00					9407	1566	1434	269	6890	2840	1330	130	—	1070	550	80
	235+00	11014	2007	903	221	7641	2641	1379	138	8630	1640	800	160	—	1900	210	70
	236+00	7034	3869	580	228	8090	2145	1228	207	7570	1800	470	170	—	1960	470	110
	237+00	7779	386	1317	186	9552	455	834	172	10110	1040	310	130	—	1010 ^c	130 ^c	90 ^c
	238+00	8441	1821	1097	214	7890	2310	1510	138	12140	2080	760	180	—	1350	270	120
	239+00	10393	814	2490	172	9055	1676	897	172	8980	4100 ^b	470	150	—	3760 ^c	100 ^c	130 ^c
	Mean CoV	8280 22.2	2370 79.3	1770 61.1	210 11.8	8490 12.1	2190 42.5	1400 26.8	180 22.3	8300 24.5	2160 30.0	910 48.5	150 13.2	—	2640 91.5	340 47.1	100 19.7

^a 1 MPa = 0.145 ksi

^b Outlier tested according to Chauvenet's criterion

^c Not considered in the average calculation because of unsatisfactory deflection bowl

E1 Modulus of HMA

E2 Modulus of lime-GGBFS soil

E3 Modulus of lime-treated subgrade

E4 Modulus of subgrade

CoV Coefficient of variation (%)

Table 3.7 Comparison of Backcalculated Moduli Computed from 28-day, 440-day, 1034-day, and 1564-day FWD Deflection Tests Lime-fly Ash Section without Drainage Layer

Section	Station	1564 - day Modulus, MPa ^a				1034 - day Modulus, MPa ^a				440 - day Modulus, MPa ^a				28 - day Modulus, MPa ^a			
		E1	E2	E3	E4	E1	E2	E3	E4	E1	E2	E3	E4	E1	E2	E3	E4
6	246+00	5676	441	607	193	6228	320	538	103	5790	350	180	130	—	220	400	140
	247+00	5483	455	772	179	6297	421	683	97	5700	420	210	140	—	370	270	120
	248+00	5283	821	621	103	5379	352	200	76	4360 ^b	350	230	80 ^b	—	220	740	70
	249+00	6828	338	1545	131	5972	497	607	124	5340	400	340 ^b	160	—	260	5240 ^b	100
	249+50	6324	690	1407	145	6097	538	703	131	5380	720 ^b	220	160	—			
	Mean CoV	5920 10.8	550 36.3	990 45.5	150 24.2	5990 6.1	430 21.8	550 37.4	100 20.7	5550 4.1	380 9.4	210 10.3	150 10.2	—	270 26.5	470 51.6	110 27.8

^a 1 MPa = 0.145 ksi

^b Outlier tested according to Chauvenet's criterion

^c Not considered in the average calculation because of unsatisfactory deflection bowl

E1 Modulus of HMA

E2 Modulus of lime-fly ash soil

E3 Modulus of lime-treated subgrade

E4 Modulus of subgrade

CoV Coefficient of variation (%)

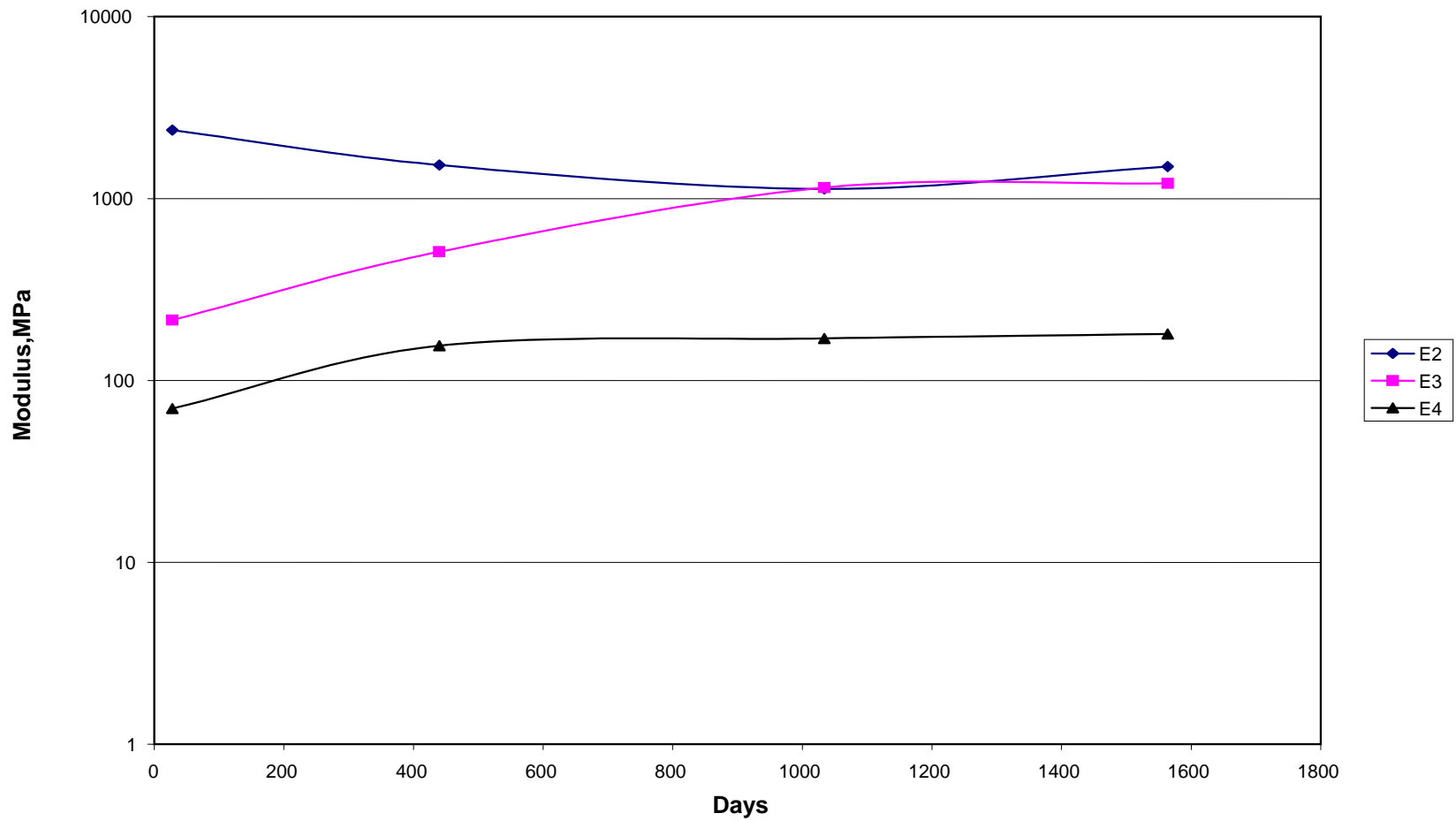


Figure 3.4 Modulus (backcalculated) increase with time of the cement-fly ash section. E_2 = Modulus of cement-fly ash soil, E_3 = Modulus of lime-treated subgrade, E_4 = Modulus of subgrade.

3.3.5 Section 5 (lime-GGBFS). As discussed in the previous section, both 1034-day and 1564-day deflection, data was analyzed with the special procedure developed with the ELMOD program. First, the modulus change from 1034 to 1564 days was not statistically significant, nor was the change from 440 to 1564 days (Table 3.6, Figure 3.5). It appears that the lime-GGBFS mix attained its full potential (2640 MPa) in 28 days or so, and more or less retained its stiffness for the first five years.

It is noteworthy that the specific ELMOD procedure resulted in backcalculated moduli of the base layer that were reasonably larger than the underlying treated subgrade (2190 vs. 1400 in 1034 days and 2370 vs. 1770 in 1564 days). A similar trend was observed with the cement-fly ash section as well, when employing ELMOD for deflection analysis. Not only did MODULUS v.5.1 and v.6 fail to discriminate between the two layers, they often resulted in modulus “reversal,” i.e., treated subgrade stiffer than the lime-GGBFS base layer.

3.3.6 Section 6 (lime-fly ash). Unable to backcalculate “reasonable” moduli with MODULUS v.6 software, both 1034-day and 1564-day data were analyzed deploying the modified ELMOD procedure, with the results tabulated in Table 3.7 and Figure 3.6. Note that the 1034-day results are somewhat different from those reported in Table 3.6 of Interim Report III. It is clear that the modulus of the lime-fly ash mix steadily increased from 28 days to 1564 days though the absolute value of the modulus was significantly lower than that of the control cement section, 550 MPa vs. 3100 MPa at 1564 days. The same deflection data were analyzed assuming a three-layer structure, combining the lime-fly ash and lime-treated layers clubbed together. Those results for two periods, listed in Table 3.7.a, substantiate the finding from the four-layer analysis that the moduli of both layers increased, specifically from 1034 days to 1564 days. The increase noted, namely, 480 MPa to 660 MPa, is in line with those observed for individual layers (see Table 3.7). It is troubling to note, however, that the modulus of lime-fly ash base lagged behind that of the lime-treated subgrade, practically throughout the five-year life of the pavement section. This result and the implications on the use of lime-fly ash in base construction will be discussed further in a later section.

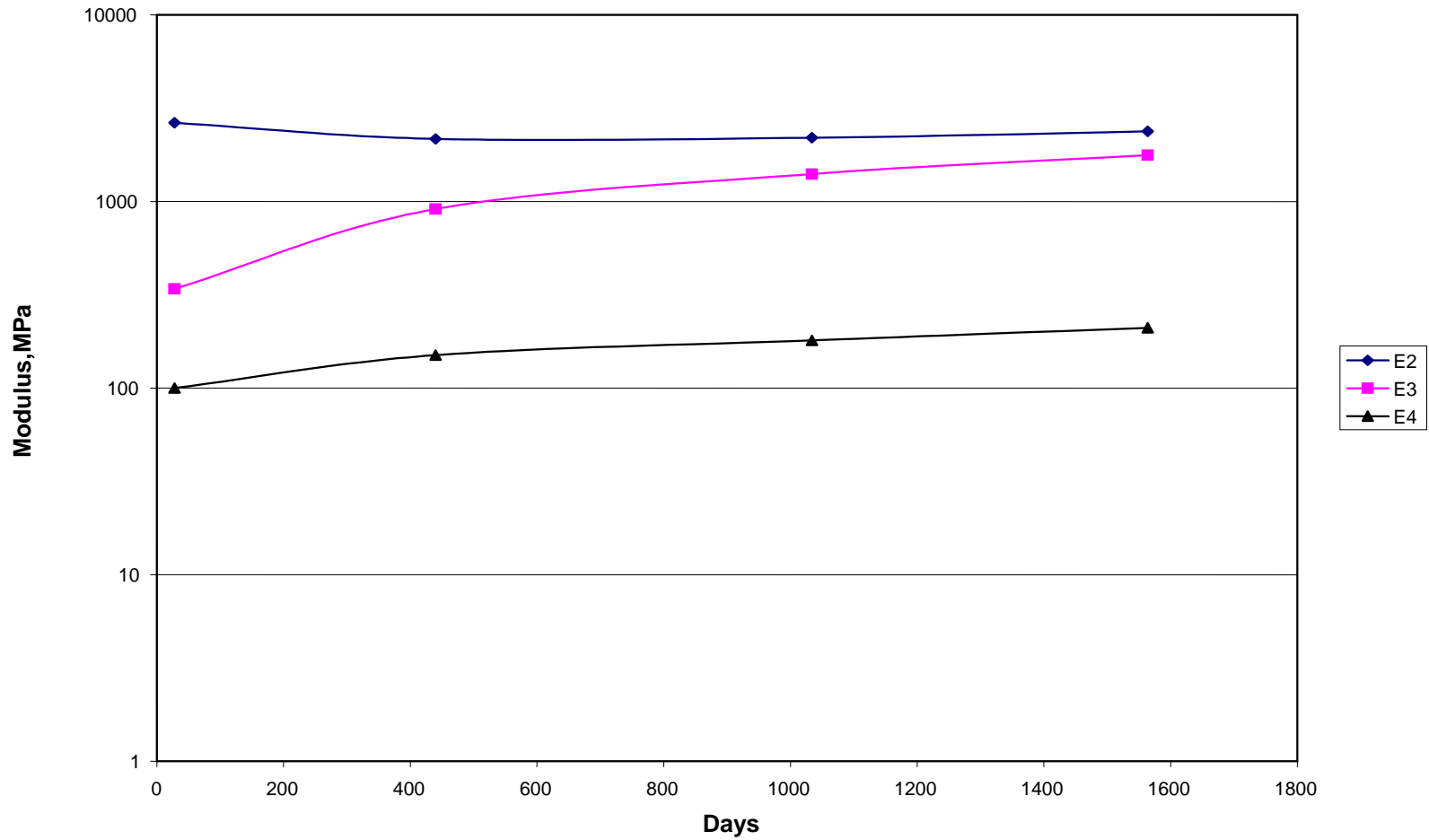


Figure 3.5 Modulus (backcalculated) increase with time of the lime-GGBFS section. E_2 = Modulus of lime-GGBFS soil, E_3 = Modulus of lime-treated subgrade, E_4 = Modulus of subgrade.

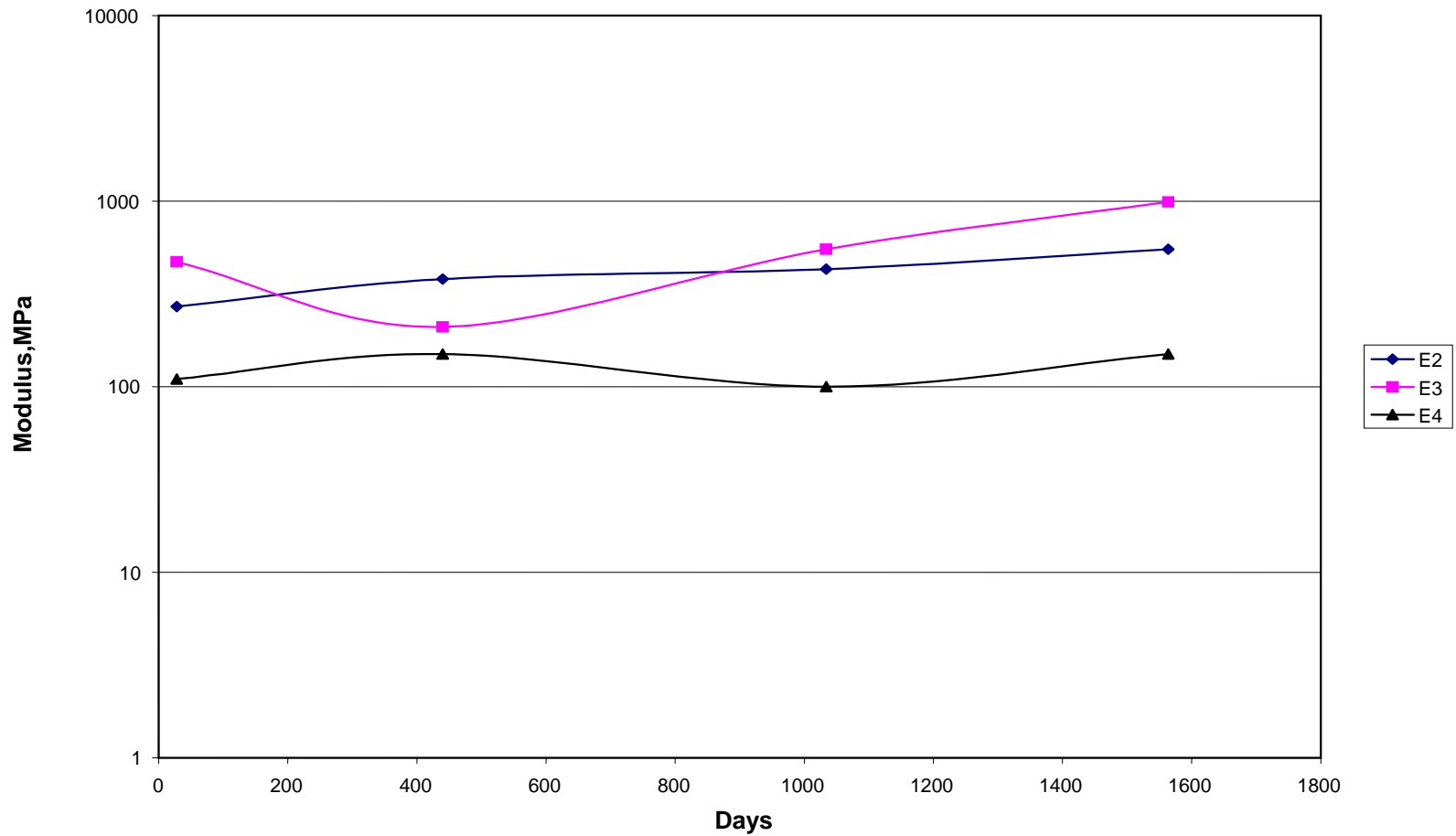


Figure 3.6 Modulus (backcalculated) change with time of the lime-fly ash section without drainage layer. E_2 = Modulus of lime-fly ash soil, E_3 = Modulus of lime-treated subgrade, E_4 = Modulus of subgrade.

**Table 3.7.a. Moduli Computed from 1034-day and 1564-day FWD Deflection Tests
Lime-fly Ash Section Without Drainage Layer Three-layer Analysis**

Section	Station	1564-day Modulus, MPa ^a			1034-day Modulus, MPa ^a		
		E1	Composite ^f	E4	E1	Composite ^f	E4
6	246+00	5471	481	197	5826	405	103
	247+00	5346	548	183	5781	549	95
	248+00	5160	710	100	5195	292	69
	249+00	6312	706	130	3457	553	119
	249+50	6163	860	150	5922	583	123
	Mean	5690	660	150	5240	480	102
	CoV	9	22.6	25.8	19.8	26	21.2

^a 1 MPa = 0.145 ksi

^f Composite modulus of lime-fly ash and lime-treated subgrade

E1 Modulus of HMA

E4 Modulus of Subgrade

CoV Coefficient of variation (%)

3.3.7 Section 6 (alternate). The presence of a drainage layer necessitated a four-layer analysis: HMA layer, drainage layer, combined lime-fly ash and lime-treated subgrade, and subgrade layer. While comparing the 440-day and 1034-day modulus, as expected the modulus of the composite layer increased from 450 to 650 MPa (Table 3.8), and this trend did not continue from 1034 to 1564 days. A comparison of the composite modulus (lime-fly ash and lime-treated subgrade) between section 6 and section 6 (alternate) is presented in Table 3.9. Comparing the moduli of both sections can determine whether the drainage layer has any effect on material performance. It is observed that the composite modulus of 6 (alternate) and that of 6 are statistically not different, which only suggests that the drainage layer at the top of the base has practically no effect. Improved drainage, however, may result in better pavement performance in the long run.

Section 6 and 6 (alternate) show nearly identical composite moduli, validating the three-layer analysis of these sections, and in turn, the observation that the lime-fly ash material is in fact less stiff than the lime-treated subgrade. Although no conclusive evidence to support this finding can be offered at this time, clearly the lime-fly ash mix fell short of realizing its full potential.

**Table 3.8 Comparison of Backcalculated Moduli Computed from 28-day, 440-day, 1034-day, and 1564-day FWD Deflection Tests
Lime-fly Ash Section with Drainage Layer LFA and Lime-treated Subgrade Combined**

Section	Station	1564-day Modulus, MPa ^a				1034-day Modulus, MPa ^a				440-day Modulus, MPa ^a			
		E1	Drainage layer ^e	Composite ^f	E4	E1	Drainage layer ^e	Composite ^f	E4	E1	Drainage layer ^e	Composite ^f	E4
6 (alternate)	25100	6883	242	855	131	7221	145	655	110	6790	160	540	120
	25200	6297	159	710	103	6910	110	538	29	6430	130	410	90
	25300	7075	386	414	124	6897	338	469	83	8420	160	270	70
	25400	5972	124	738	200	6710	117	917	145	8030	170	590	150
	Mean CoV	6560 7.8	230 51.2	680 27.6	140 30.1	6940 3.1	180 60.9	650 30.6	110 53.3	7420 12.9	160 11.2	450 31.7	110 32.6

^a 1 MPa = 0.145 ksi

^e Modulus of drainage layer

^f Composite modulus of lime-fly ash and lime-treated subgrade

E1 Modulus of HMA

E4 Modulus of Subgrade

CoV Coefficient of variation (%)

Table 3.9 Composite Modulus Comparison Between Sections 6 and 6 (Alternate) of 1564-day and 1034-day FWD Deflection Tests

Section	Station	1564-day Composite Modulus ^f , MPa ^a	1034-day Composite Modulus ^f , MPa ^a
6	246+00	481	405
	247+00	548	549
	248+00	710	292
	249+00	706	553
	249+50	860	583
	Mean	660	480
6 (alternate)	251+00	855	655
	252+00	710	538
	253+00	414	469
	254+00	738	917
	Mean	680	650

^a 1 MPa = 0.145 ksi

^f Composite modulus of lime-fly ash and lime-treated subgrade

3.4 Lime-treated Subgrade

Investigating the modulus of lime-treated subgrade from sections 1 through section 6, two graphs are plotted with the station-wise modulus (Figure 3.7), and section-wise modulus (Figure 3.8). In view of the identical lime-treated subgrade in all of the sections, the variation observed from beginning to end of the test road is substantial, as per the 440-day and 1564-day results (Figure 3.8). For example, the modulus of the lime-treated subgrade remained nearly constant or decreased slightly from section 1 to 4, increased in section 5, and dropped substantial in section 6. The drastic decrease of the modulus in section 6 is due in part to the relatively weak pavement structure resulting from the fragile LFA base. Though not theoretically proved, it is our observation that if one of the layers in a pavement structure turns out to be weak (LFA base in this case), the adjoining layer(s) (HMA and lime-treated subgrade) would show apparent weakness as well.

Note that the LFA base modulus was even lower than that of the lime-treated subgrade, due in part to poor mixing of the additives. It could be that the partially cemented LFA base attracted surface water soaking up the pavement, including the lime-treated subgrade. A trend in the variation from the norm in lime-treated subgrade—low modulus values—was observed in sections 4 and 6 where the stabilized base showed marginal stiffness gain, causing its modulus to lag behind that of the treated subgrade. Another implication is that the backcalculation of section 6 and possibly section 4, could have been affected by the anomalies associated with an “inverted” pavement configuration.

3.5 Hot Mix Asphalt Surface

Making use of the backcalculation results, the spatial variation of the HMA modulus was also investigated. Though the moduli of the HMA and subgrade were obtained from four-layer analysis, those results were substantiated with three-layer analysis results. As can be verified in Figure 3.9, HMA modulus remains practically constant for sections 1, 2, 3, and 5, with a minor reduction in sections 4 and 6 (alternate), and section 6 showing substantially low HMA modulus. This low modulus can be attributed to the increased deflections/strains and accompanying nonlinear behavior of AC. On the average a 70% increase in HMA strain is observed from control section to lime-fly ash section for a FWD load of 17,000 lb, owing primarily to decreased base support. The increased strain not only triggers nonlinear behavior but also promotes fatigue damage in HMA, and in turn, diminishes its stiffness modulus.

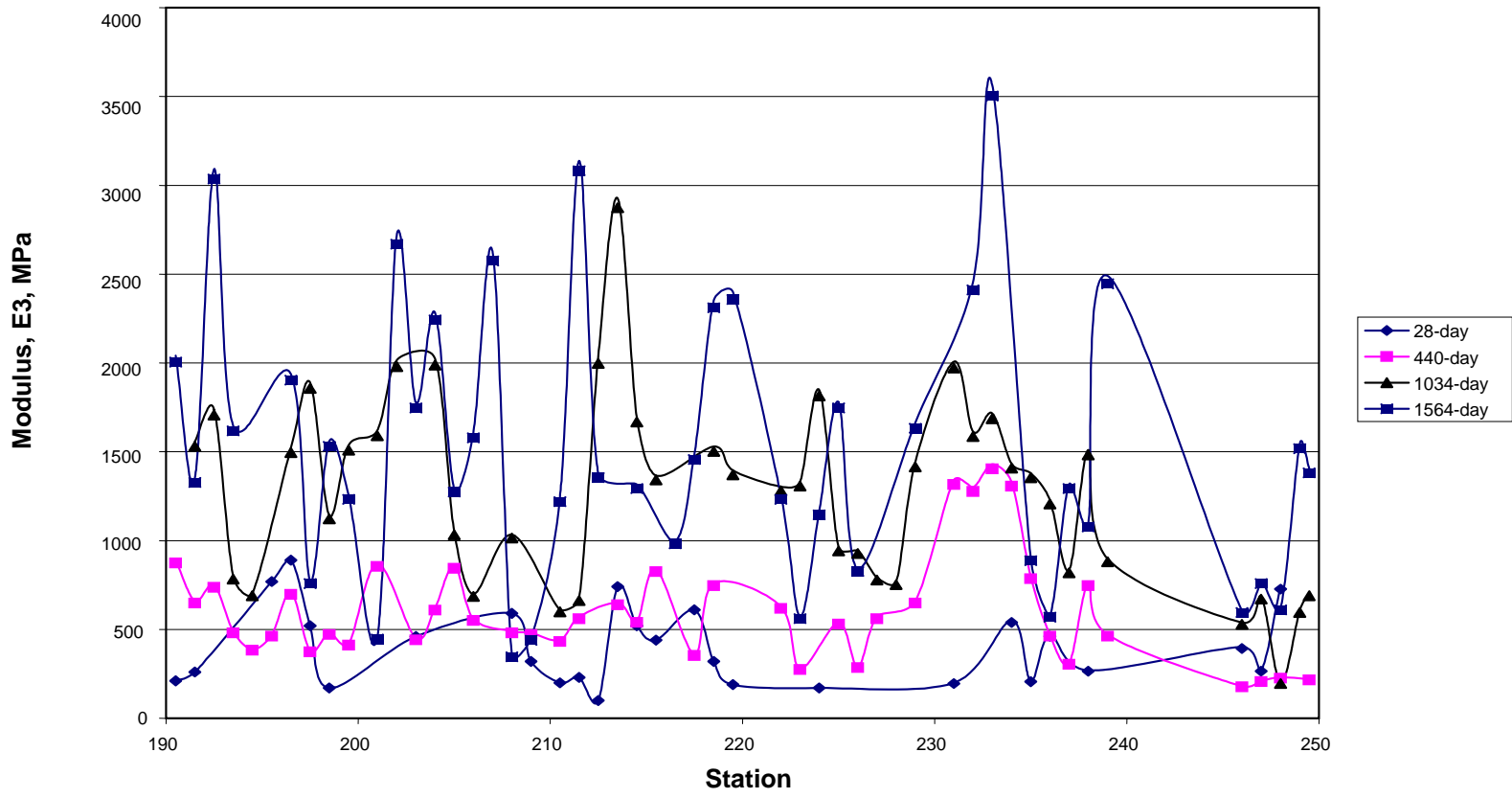


Figure 3.7 Modulus (backcalculated) variation of lime-treated subgrade, E3, along the road.

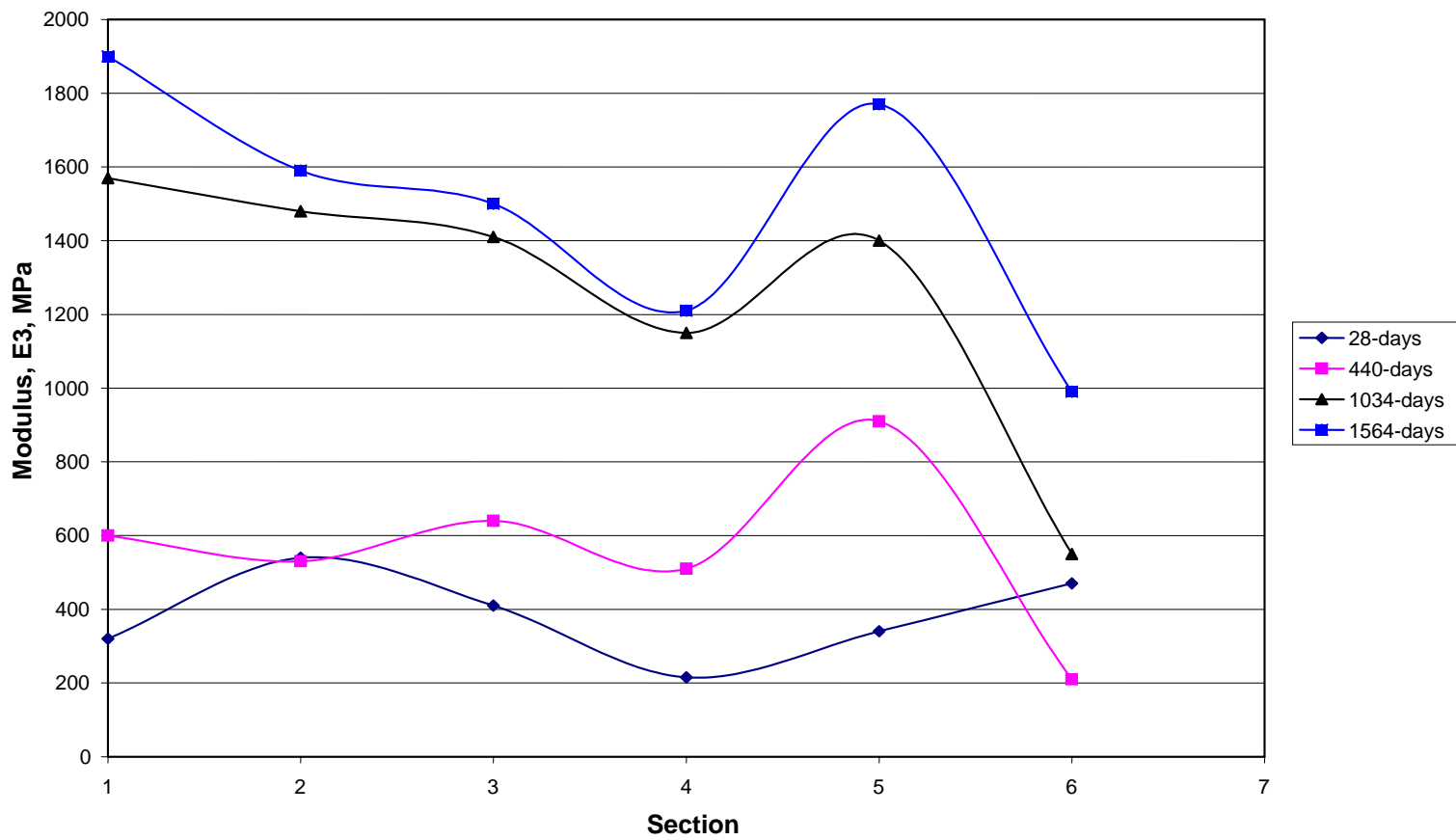


Figure 3.8 Modulus (backcalculated) variation of lime-treated subgrade, E3 (section average).

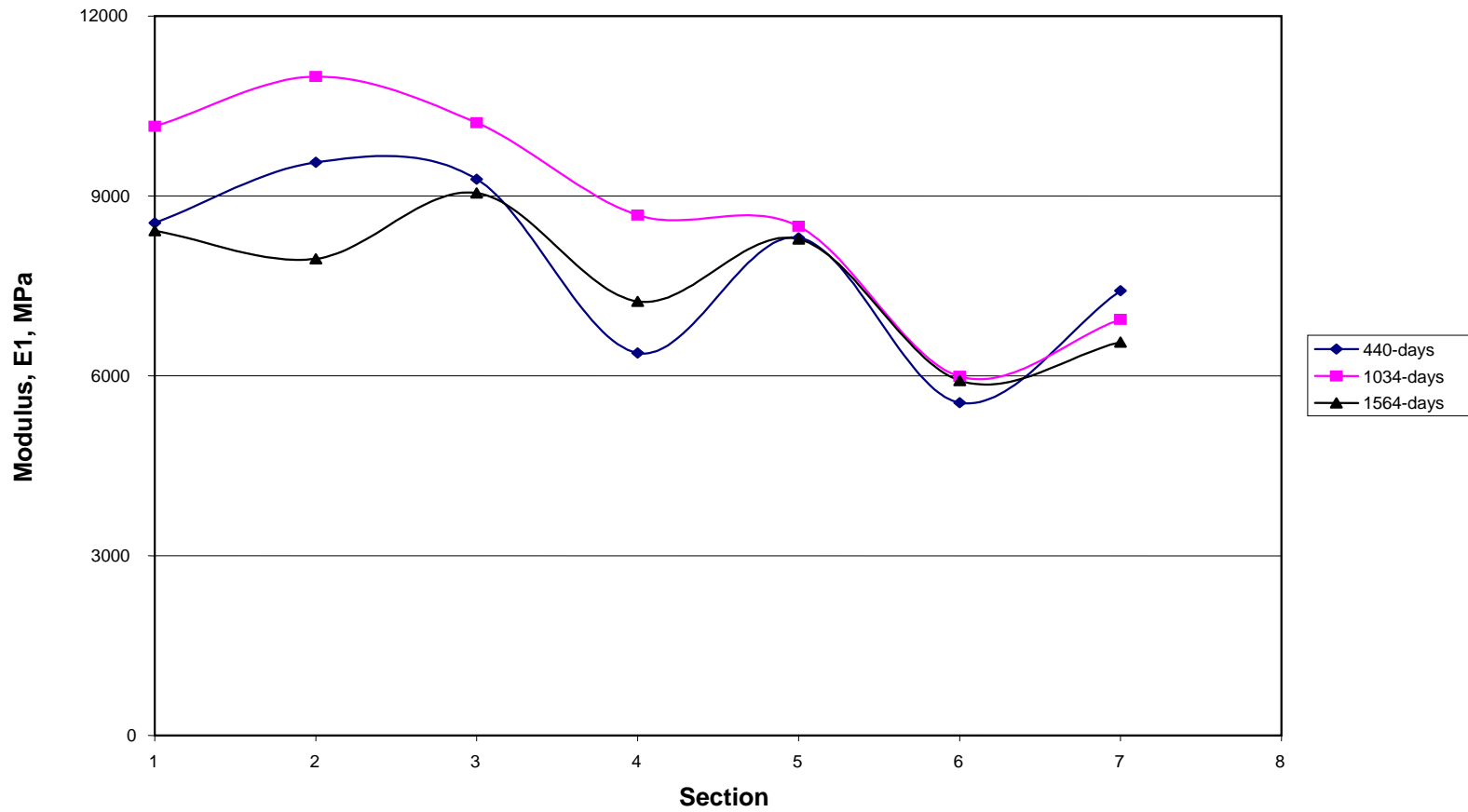


Figure 3.9 Modulus (backcalculated) variation of hot mix asphalt, E1 (section average).(7 refers to section 6 [alternate]).

Chronologically, the HMA modulus increased from 440 days to 1034 days and subsequently decreased during the period from 1034 days to 1564 days, though the change was minor during both periods. Remember that both 440-day and 1564-day tests were conducted during cold weather, mandating a temperature correction decreasing the backcalculated modulus to arrive at a standard temperature-modulus. A brief description of the temperature correction methodology can be seen in Appendix B (Lukanen, Stubstad and Briggs 2000). An opposite correction was implemented in the 1034-day modulus, as the FWD tests were conducted during warm weather. Admittedly, possible errors (for example, temperature measurement of the pavement and BELLS 3 equation itself) could have been factors biasing the corrected HMA modulus. Evidence is lacking to suggest that HMA stiffness had altered over the three-year period of trafficking.

3.6 Subgrade

Figure 3.10 depicts the spatial variation of the subgrade modulus. Discounting for one set of moduli at 28 days, the variability from section 1 to section 4 is statistically not significant. The section 5 subgrade modulus increased, followed by sections 6 and 6 (alternate), whose moduli decreased significantly. As alluded to before, the overall strength of the pavement in some way affects the backcalculation results resulting in an underprediction or overprediction of layer modulus. Weaker pavements tend to predict lower modulus, and stronger pavements show higher modulus. Note that all three layers of the LFA section – HMA, lime-treated subgrade, and subgrade – exhibited relatively low moduli in comparison to those in the other five test sections. Chronologically, average subgrade moduli steadily increased from 100 MPa in 28 days to 160 MPa in 1564 days. Lime leaching from the lime-treated upper layer modifying the subgrade could be the primary reason for this modulus increase over the five-year period. The backcalculated subgrade moduli of the six test sections at 1564 days are compared with those derived from Dynamic Cone Penetration test results in a later section.

3.7 Pavement Cores

Cores were cut from each section – two cores from each of the short sections and three from each of the full sections. A 102-mm (4-in.) diameter drill was employed to cut through the top asphalt layer (design depth 220 mm [8.75 in.]) to reach the stabilized layer (design depth 150 mm [6 in.]), retrieving the samples for unconfined compressive strength (UCS). Another purpose of coring was to determine pavement layer thicknesses to facilitate the backcalculation analysis of layer moduli.

Prior to presenting the strength results, included in this section is a visual examination of the cores from the base layer. The core rating scheme developed by Barstis (Barstis 2003) recognized condition rating from 1 to 6, one representing intact samples with smooth cut face and six denoting a broken sample making it impossible to perform any physical measurement. All of the 21 cores were classified according to this scheme, and the relative quality is denoted in column 2 of Table 3.10. Note that 43% of the cores rated 1, 38% rated 2, 9% rated 3, and the remaining 10% rated 6. Two attempts to retrieve cores in section 6 (alternate) were unsuccessful. Note that the precut core retrieval of the entire project was 83%.

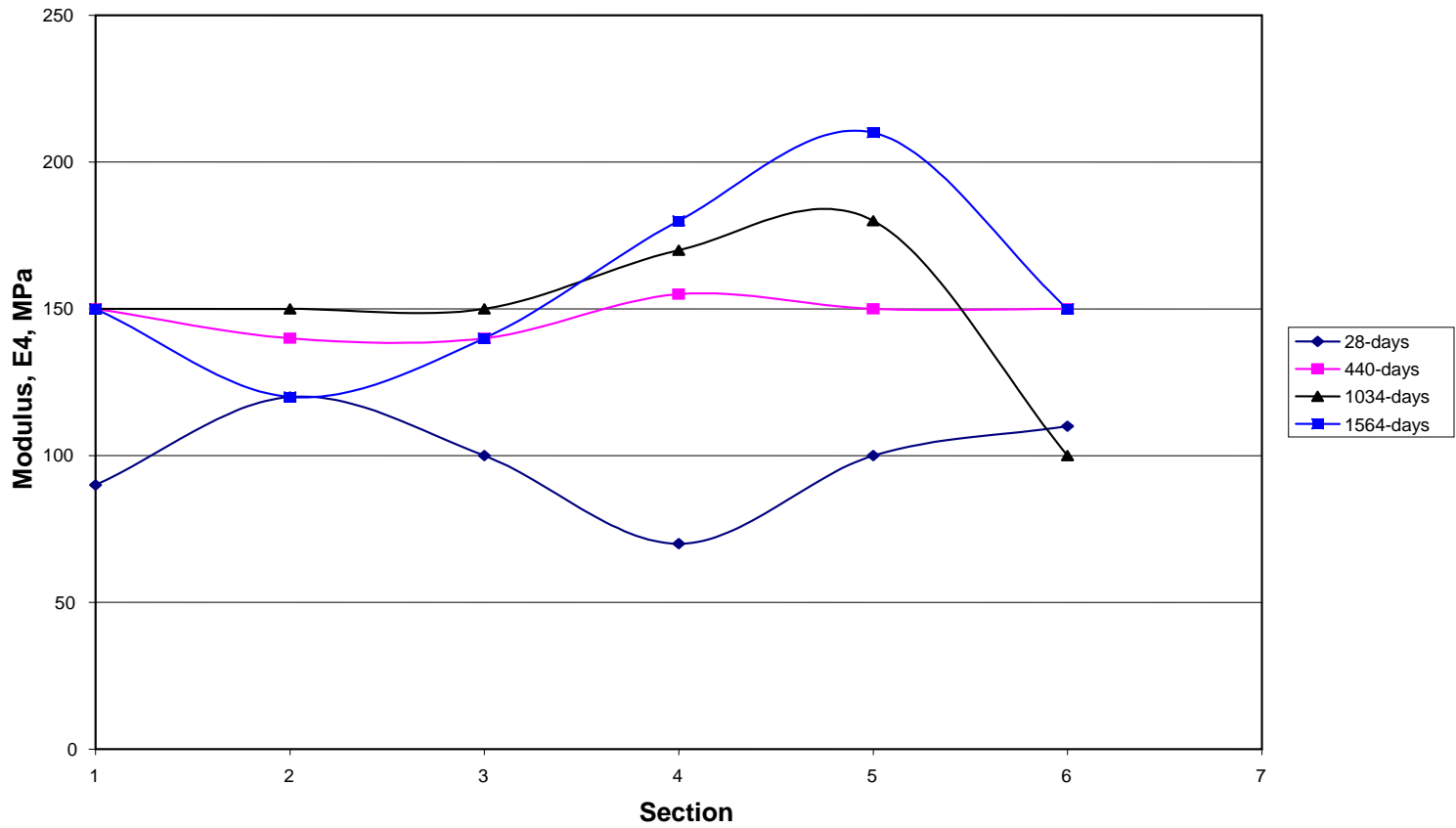


Figure 3.10 Modulus (backcalculated) variation of subgrade, E4 (section average) (7 refers to section 6 [alternate]).

The HMA and stabilized base layer thicknesses for each of the cored locations are recorded in columns 3 and 4, respectively, of Table 3.10. All of the test locations showed HMA in excess of the 220 mm (8.75 in.), with the maximum thickness measured being 260 mm (10.0 in.). The stabilized layer thicknesses range from a low of 110 mm (4.6 in.) to a high of 170 mm (6.8 in.). The bottom ends of a few extracted stabilized base cores were poorly cemented and, therefore, washed into the hole, especially CFA and LFA cores. Inadequate mixing and/or deficiency of the stabilizing agent seemed to be the reason for the poorly cemented material at the bottom. Note that at some locations a significant difference exists between the in-situ layer thickness and the height of the retrieved sample, due in part to the partial disintegration of core samples.

Out of the 21 cores, only one core had a preexisting crack, and that was in the LFA section at station 248+00. As pointed out, despite two attempts in section 6 (alternate), both cores were completely disintegrated by the grinding action of crushed rock from the drainage layer.

3.7.1 Unconfined Compression Strength (UCS). Out of the 19 cores, only four cores required capping with plaster of paris. The remaining 15 cores were trimmed with a saw ensuring end surfaces perpendicular to the axis of the core. The height of each core after preparation but before compression testing is listed in column 6 of Table 3.11. The density of the core sample was determined in accordance with AASHTO Designation T 166-78 (1982) and listed in column 4 of Table 3.12. Moisture content tabulated in column 3 was determined by the standard gravimetric procedure for which samples were collected after compression testing. The cores were tested in compression at a strain rate of 0.049 in./minute and the results tabulated in column 5 of Table 3.11. Most, if not all, of the cylinders broke in the “split mode,” as opposed to the typical shear failure (inclined failure plane), attributable to height-to-diameter ratio being smaller than 2.

Because the UM laboratory mixture design was based on samples of height-to-diameter ratio 2, all of the core strengths were normalized for comparison purposes. The equation for the correction factor is based on the premise that Proctor strengths are generally 30% higher than that of samples with a height-to-diameter ratio of 2. Assuming a linear interpolation of strength between the ratios 2:1 and 1.15:1, the following equation was developed:

$$\text{Correction Factor} = 0.77 + 0.27 (2-H/D) \quad (3.1)$$

where H/D = height-to-diameter ratio of the tested sample

The corrected strength of each sample can be seen in column 9 of Table 3.11

3.7.2 Unconfined compressive strength comparison. As expected, core strength of all of the sections increased from 28 to 440 days and to 1564 days (see Table 3.11). The five-year increase ranges from a low of 78% for precut cement to a high of 171% for lime-GGBFS. Other noteworthy observations include:

Table 3.10 Thicknesses of HMA and Core Samples, and Classification of the Litter

Section	Station	HMA Thickness(inches)	Base Thickness(inches)	Core Classification
1A	190+50	10.0	5.5	2
	194+50	9.5	5.9	3
3A	210+50	9.0	6.0	1
	214+50	9.6	4.6	2
1B	195+50	9.3	5.8	1
	199+50	9.8	5.8	2
3B	215+50	9.3	6.3	2
	219+50	9.8	6.0	1
2	201+00	9.3	5.8	1
	203+00	9.2	5.0	2
	209+00	8.9	5.3	1
4	221+00	10.0	6.8	1
	223+00	9.5	5.5	2
	229+00	9.6	5.8	2
5	231+00	10.0	6.0	1
	233+00	9.0	5.3	1
	239+00	9.4	4.8	1
6	247+00(1) ^a	-	-	6
	247+00(2)	9.3	4.5	3
	248+00(1) ^a	-	-	6
	248+00(2)	9.3	4.5	2
6(alternate)	251+00(1) ^a	-	disintegrated	
	251+00(2) ^a	-	disintegrated	

^a Base core could not be retrieved

Table 3.11 Properties of Core Samples and Unconfined Compressive Strength at 1564 Days, Corrected to 2:1 Height-to-Diameter Ratio

Section	Station	1564 days							Average Strength at 440-day(kPa)	Average Strength at 28-day(kPa)	
		Moisture Content (%)	Dry Density (lb/ft ³)	Compressive Strength (kPa)	Height (inch)	H/D ratio	Correction factor	Corrected Strength (kPa)			Average Strength (kPa)
1A	190+50	17.8	111.3	1876	5.6	1.41	1.2058	1556	1730	1670	710
	194+50	18.1	106.9	1596	5.6	1.43	1.1996	1330 ^a			
3A	210+50	15.6	112	3054	5.6	1.42	1.2031	2538			
	214+50	16.2	109.3	1417	4.5	1.14	1.3000	1090			
1B	195+50	12.9	117.5	3700	5.7	1.45	1.1943	3098	2630	1910	1070
	199+50	14.8	112.8	2731	5.5	1.39	1.2165	2245			
3B	215+50	15.6	109.5	2029	6.2	1.57	1.1497	1765			
	219+50	18.5	107.9	4074	5.8	1.46	1.1889	3427			
2	201+00	17.8	109.4	2775	5.2	1.33	1.2360	2245	3370	2370	880
	203+00	17.2	112.7	5241	3.8	0.96	1.3640	3842			
	209+00	15.2	112	5037	5.1	1.29	1.2503	4029			
4	221+00	18.7	111.9	5372	6.8	1.71	1.0999	4884	3270	2470	910
	223+00	15.9	113.6	2566	4.4	1.13	1.3053	1966			
	229+00	14.5	116.6	3536	5.7	1.45	1.1915	2968			
5	231+00	12.7	119	7650	5.6	1.42	1.2031	6359	5730	3720	1390
	233+00	12.5	122.1	8137	5.5	1.41	1.2085	6733			
	239+00	13.8	118.6	5287	4.6	1.18	1.2885	4103			
6	247+00	18.7	108.2	1240	3.5	0.90 ^b	1.3866	894	1280	910	240
	248+00	15.8	100	3540	3.5	0.90 ^b	1.3866	2553			

^a Not considered in the average calculation because of a chip in the sample

^b Core diameter 3.875 in.; remaining cores 3.937 in.

- Though the precracked section core strength at 28 days was comparable to that of the control section (1A, 3A), it surpassed the latter's strength at 440 days and even more so at 1564 days. This result clearly suggests that, despite the precracked material suffering a temporary strength loss for having induced microcracks, it regained strength 169% and 220% over the 440-day and 1564-day periods, respectively. Backcalculated moduli also showed a similar increasing trend, but less pronounced.
- The strength of cement-fly ash mix was coincidentally identical to that of the precracked cement in all three testing periods – 28 days, 440 day, and 1564 days. During the five-year period, however, its strength gain is only second to the lime-GGBFS mix (3380 kPa vs. 8620 kPa in 1564 days). The 28-day strength of CFA mix is comparable to that of the control cement; however, during the five-year period the CFA strengths surpassed that of the control mix by 117%. The low early strength fruiting to high ultimate strength is desirable in regard to alleviating shrinkage cracks.
- Lime-GGBFS appears to be the predominant strength gainer at 28 days, 440 days, and also at 1564 days. Starting out with a strength of 1390 kPa (200 psi), it soared to 8620 kPa (1250 psi) in five years, unlike any other mix. It would be fair to conclude that the admixture percentage – namely, 2% lime and 6% GGBFS – is on the high side, resulting in a high-strength material, a little more than two times the design strength (2410 kPa vs. 5730 kPa). A recommendation may be to consider reducing the additive percentage.
- That the LFA mixture exhibits a strength of only 1280 kPa, despite a substantial increase from 240 kPa in 28 days, raises some concern that its effectiveness in all of the soil materials cannot be taken for granted. Considering that only the top 9 cm (3.5 in.) of the material survived the coring operations (with water) suggests that the lower half of the LFA mix is fragile, undermining the structural capacity of the pavement.
- Though two undersized cores survived during the 440-day coring, two attempts in section 6 (alternate) at 1564 days did not produce intact samples. The material was so weak that the stone pieces infiltrated from the drainage layer on top resulted in a complete disintegration of the lime-fly ash material.

3.7.3 Unconfined Composite Strength (UCS) affected by uneven mixing. The consequences of uneven mixing, both spatially and through the depth, include structural deficiency and large spatial variation of UCS. If the distribution of the stabilizing agent is uneven from top to bottom, invariably with more at the top, the cutting of cores with water would result in erosion of bottom unmixed material, and in turn, relatively high strength for the retrieved top portion. This seems to have been clearly the case of the LFA core at station 248+00. With this in mind, a weighted average of the two samples at 247+00 and 248+00 is calculated (1280 kPa), rather than a simple average (see column 10, Table 3.11).

One core sample in the CFA section and yet another sample in the LGBFS section also suffered excessive erosion of the lower portion of the sample, due in part to uneven distribution of stabilizing agents from top to bottom. Therefore, uneven mixing has been a problem when multiple stabilizing agents were stipulated, for example, cement and fly ash. A recommendation would be to pay special attention to enforcing the quality assurance procedures.

3.8 Dynamic Cone Penetration (DCP) tests. The DCP device deployed in this investigation utilized an 8-kg (17.6-lb) hammer dropping through a height of 57.6 mm (22.6 in.). A 60° apex angle cone was the standard in the device.

After removing the HMA core and the stabilized base core beneath, the holes were cleaned with a shop wet-vacuum, in preparation for the DCP test. The lime-treated subgrade (nominal thickness 152 mm [6 in.]) and the underlying subgrade were tested to approximately 500 mm (20 in.) depth. Typical penetration vs. number of blows of two of the test sections are graphed in Figures 3.11 and 3.12. Thickness of the lime-treated subgrade at each location was estimated from the change in slope of the top portion of the curve and is tabulated in column 3 of Table 3.12. Column 4 presents the Dynamic Cone Penetration Index (DCPI in mm/blow) of the treated subgrade. Making use of the empirical equation 3.2 (McElvancy and Djatinka 1991), the UCS of the lime-treated subgrade is calculated and listed in column 5.

$$UCS = A (DCPI)^{-1} + B \quad (3.2)$$

where UCS = Unconfined compressive strength, kPa; and
A, B, C, D = Regression coefficients

Another equation, equation 3.3 (Jianzhou, Mustaque and LaTorella 1999), is employed to estimate the elastic modulus of the subgrade from the DCPI (column 6), which is tabulated in column 7 of Table 3.12.

$$M_R \text{ (MPa)} = 338 (DCPI)^{-0.39} \quad (3.3)$$

where DCPI = dynamic cone penetration index, mm per blow

The thickness of the lime-treated subgrade, as determined from DCP tests, varies over a range – 127 mm (5 in.) to 165 mm (6.5 in.) – with an average value of 144 mm (5.7 in.) c.f. to the design thickness of 152 mm (6 in.). The thickness deficiency could be attributed to inadequate mixing of lime and soil. As in the case of the stabilized base, inadequate (shallow) mixing resulted in nonuniform lime distribution with depth, with little or no lime at the bottom of the layer. The UCS estimated from DCPI (average strength 930 kPa) is considered reasonable, as MDOT design calls for a CBR of 20 for treated subgrade. Note that the average M_R (backcalculated) of the lime-treated base was 1490 MPa. Based on the strength and elastic stiffness, it is construed that the lime-treated layer is expected to provide a firm foundation/capping for the pavement.

The subgrade elastic modulus (E_{back}), calculated from DCPI employing equation 3.3, is listed in column 7 of Table 3.12. Comparing these moduli with the backcalculated subgrade moduli (Tables 3.1 to 3.6), overall the DCPI-based moduli are underpredicted, by an average of 27%. Excluding the subgrade moduli predicted by the ELMOD program in sections 4 and 5, the average MODULUS v.6-based moduli of sections 1A, 3A, 1B, 3B, 2, and 6 are reasonably close to the average calculated from DCPI.

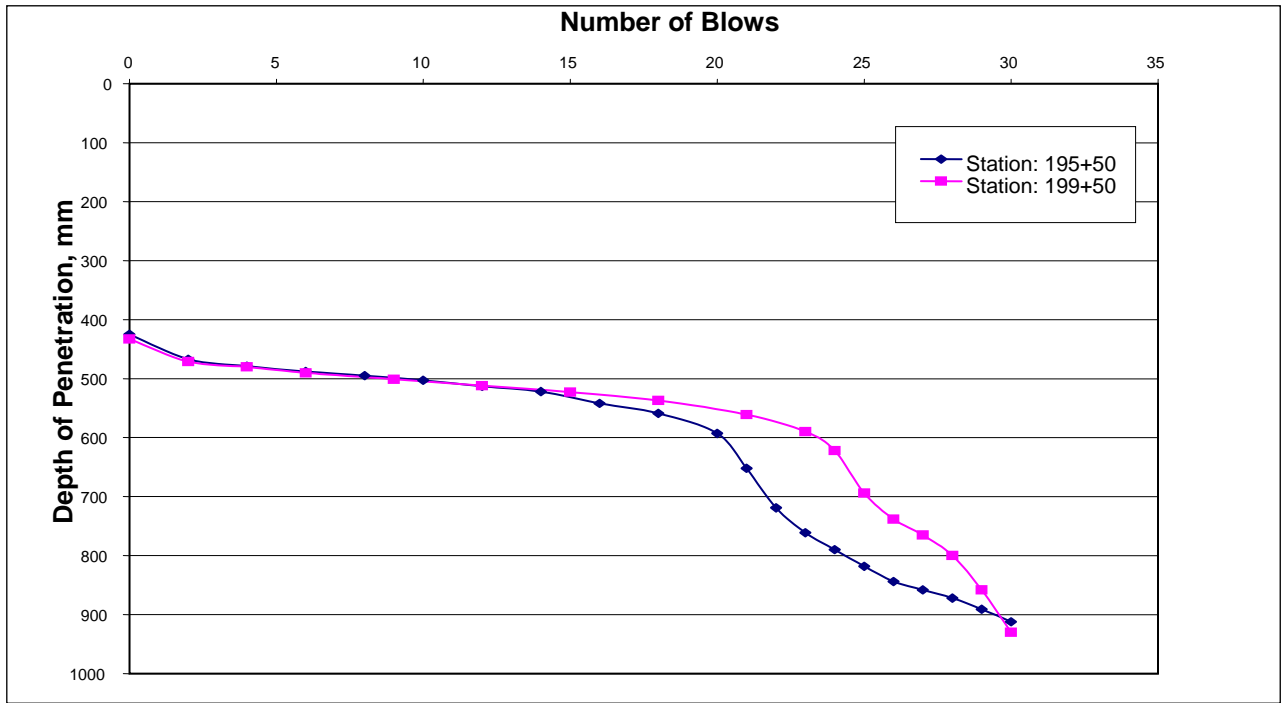


Figure 3.11 DCP test results in section 1B, Hwy #302, Marshall County.

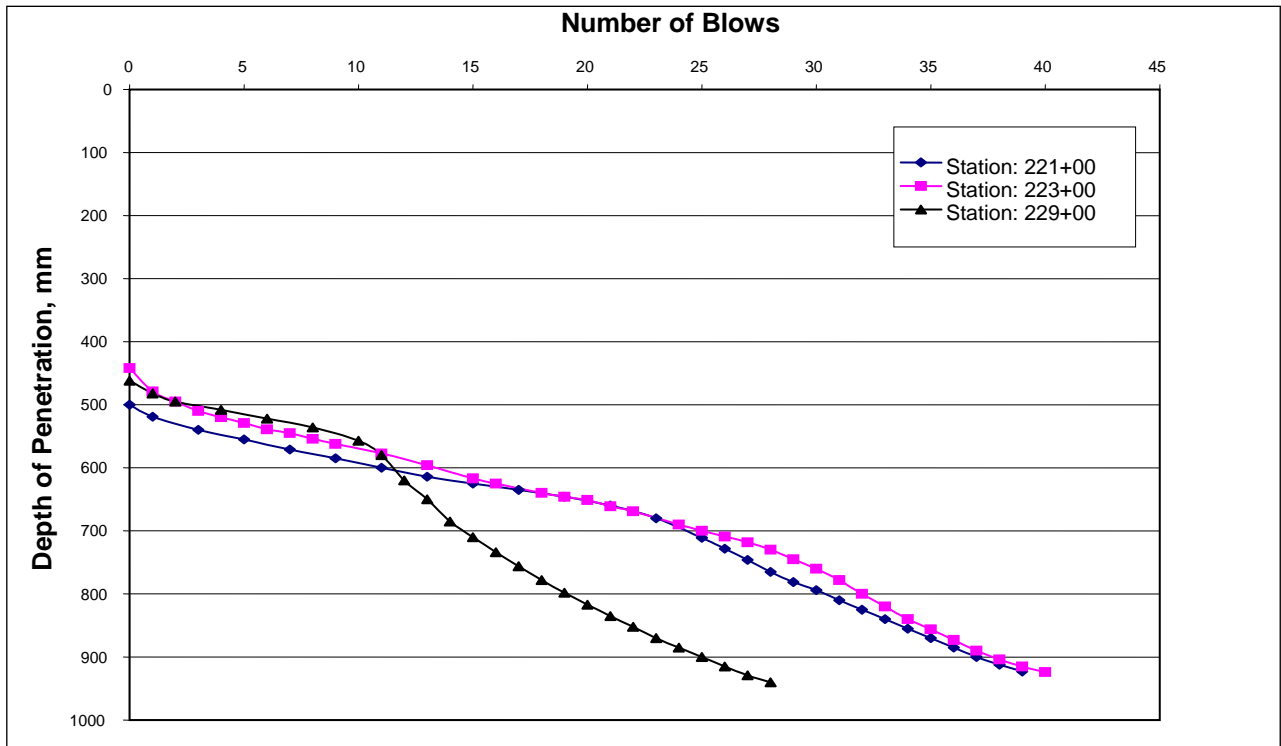


Figure 3.12 DCP test results in section 4, Hwy #302, Marshall County.

Table 3.12 Dynamic Cone Penetration (DCP) Tests Results Unconfined Compressive Strength (UCS) of Lime-treated Subgrade and Resilient Modulus (M_R) of Subgrade from Respective DCP Indices

Section	Station	Thickness of lime-treated subgrade, inches	DCPI of lime-treated subgrade, mm/blow	UCS of lime-treated subgrade, kPa	DCPI of subgrade, mm/blow	M_R of subgrade, MPa
1A	190+50	5.2	3.8	1590	8.8	140
	194+50	5.2	4.8	1330	45.7	80
3A	210+50	5.0	6.2 ^a	1080	19.4	110
	214+50	5.6	4.5	1400	5.2	180
1B	195+50	5.8	6.8	1010	35.4	80
	199+50	5.3	8.2	870	35.0	80
3B	215+50	6.0	8.4 ^a	860	4.8	180
	219+50	6.0	19.1 ^a	450	9.0	140
2	201+00	6.0	21.3 ^a	410	34.7	90
	203+00	6.3	8.9	820	17.7	110
	209+00	5.5	7.8 ^a	910	26.9	90
4	221+00	6.5	6.8 ^a	1010	14.6	120
	223+00	6.1	9.3	790	11.8	130
	229+00	5.0	10.7	710	22.5	100
5	231+00	5.9	9.1 ^a	800	15.4	120
	233+00	6.0	5.5	1190	11.6	130
	239+00	5.6	14.3	570	30.4	90
6	247+00	5.5	5.9	1130	19.5	110
	248+00	5.5	10.2	730	21.9	100
	Mean	5.6	9.0	930	20.5	110

^a DCPI applies to lower part of lime-treated subgrade(upper part got attached to stabilized base)

3.9 Summary

This chapter presents the analysis of field-test data, discussing whether the stabilized soil in each section has improved in stiffness and strength as a result of continued pozzolanic action. From 28 days onward, all of the stabilized bases except the CFA base improved so far as modulus was concerned. Though the CFA section though showed improvement up to 440 days, its modulus leveled off beyond that period. Despite relatively low modulus values, the LFA section showed stiffness gain over the five-year period. The strength gain of all of the different materials was systematic and continuous except for the control cement mixture which tended to reach a plateau between 1034 and 1564 days. The modulus of the lime-treated subgrade continued to increase with time, though the modulus of this layer beneath LFA fell short of the rest of the one mile stretch (990 kPa vs. 1590 kPa). A noticeable decrease in the HMA modulus in the LFA section was observed as well.

The thickness of the HMA layer exceeded the design thickness of 222 mm (8.75 in.), whereas the stabilized base thickness fell short of the design thickness (on average 5.5 in. vs. 6 in.). The lime-treated subgrade also showed on average a half-inch thickness deficiency, as determined by the DCP test. The UCS of the lime-treated subgrade estimated from the DCP index was basically uniform from section to section, as was the resilient modulus of the subgrade.

CHAPTER 4

PRECRACKING DAMAGE INVESTIGATED EMPLOYING MODAL ANALYSIS

4.1 Introduction

In the previous section, it is noted that the precracked layer had undergone microcracking during intentional vibrating with a roller. It was premised that the microcracks introduced would alleviate detrimental shrinkage cracks, which it did, as revealed by the crack survey results of section 2. The modulus of test section 2 before and after precracking is plotted in Figure 4.1. As a result of precracking, the cement-treated material is perceived to have undergone microcracks, with the material suffering a temporary decline in stiffness. Field monitoring indicated that the stiffness decline was not permanent. On the contrary, it recovered with time, as cement hydration continued. A laboratory study was designed to substantiate the “crack healing” and recovery hypothesis. The technique employed here is known as modal analysis, a process whereby we describe a structure in terms of its natural characteristics: frequency, damping, and mode shapes. In the case of simple structural elements, such as beams, their natural frequency affords an explicit method for characterizing the dynamic flexural moduli.

The experiment will simulate microcracks (damage) in the material, with a monitoring plan to track stiffness gain with time. Duplicate beam specimens, 287 mm long and 76 x 51-mm cross section, were cast from cement-treated material (5.5% cement). One beam was subjected to precracking and the other preserved as control beam for comparison. The time-dependent stiffness change (gain) of each beam was monitored by modal analysis, yielding natural frequencies and, in turn, modulus. The basic premise of this approach is that the presence of cracks (damage) results in a decline in natural frequency, which is directly related to modulus. The results presented in this chapter can be seen in reference 19 (George, Brajacharya and Gaddam 2002).

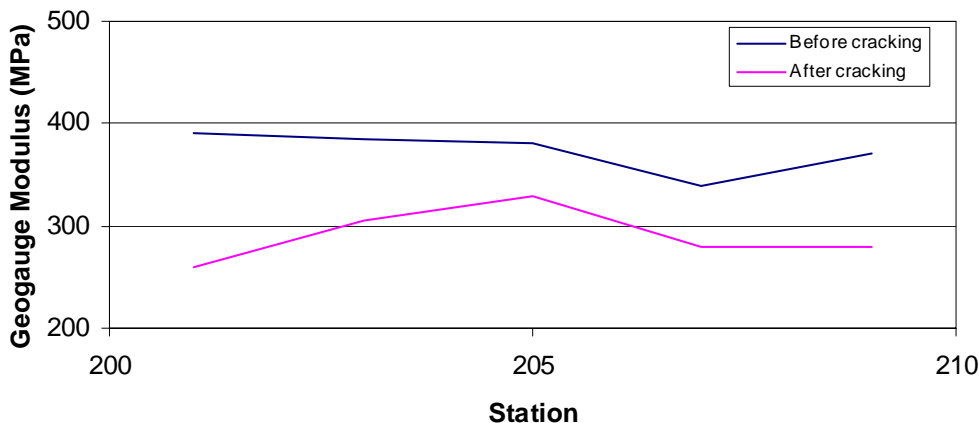


Figure 4.1: Modulus before and after precracking (adapted from reference 14).

4.2 Sample Preparation

As indicated, the beams 287 mm long with a rectangular cross section were subjected to modal impact testing. These beams were cast in accordance with ASTM D 1632-87 (with slight modification) from soil aggregate, and mixed thoroughly with the appropriate amount of cement and water. After a 24-hour moist curing, the beam scheduled to receive precracking was subjected to vibration for 7 to 10 minutes while confined in the steel mold. The table, vibrating at 10 Hz and meeting the specifications of the ASTM D 2049 test, was utilized to induce microcracks. The 7-minute vibration was repeated after 48 hours, and the precracked and control beams were moist-cured for a total of 3 days before subjecting them to vibration tests, with the tests repeated at 7, 14, and 28 days in order to monitor the stiffness recovery with time.

4.3 Experimental Setup for Vibration Study

As illustrated in Figure 4.2, the beam sample was suspended in the free-free configuration by thin nylon threads. The point of attachment is one-fifth L from the free end, a position that is in proximity to the modes of the first and second flexural modes of a Bernoulli-Euler beam. Note that the exact locations of these modes fall at $0.2241L$ and $0.1322L$, respectively, from the free end. The acceleration response of the sample was monitored by a miniature accelerometer with the sensitive axis normal to the x - z plane. The accelerometer was halfway along the width of the beam so as to minimize the influence from torsional vibration. The sample was then set into free vibrations in the x - y plane by means of an impulse along the y -direction, via an impact hammer instrumented with a force transducer. During the test, the response of the beam and the excitation force were filtered, amplified, and recorded by a dynamic signal analyzer. Discrete Fourier Transform was subsequently performed on the captured signals to produce the frequency response function (FRF). In order to substantiate the results, the beam was rotated 90° along the x -axis and the vibration test repeated. A typical FRF of a control beam sample is shown in Figure 4.3. Two peaks corresponding to the first two damped flexural vibration frequencies clearly can be observed. The damping ratios ζ of the corresponding vibration modes also are indicated and are determined by using the half-power bandwidth.

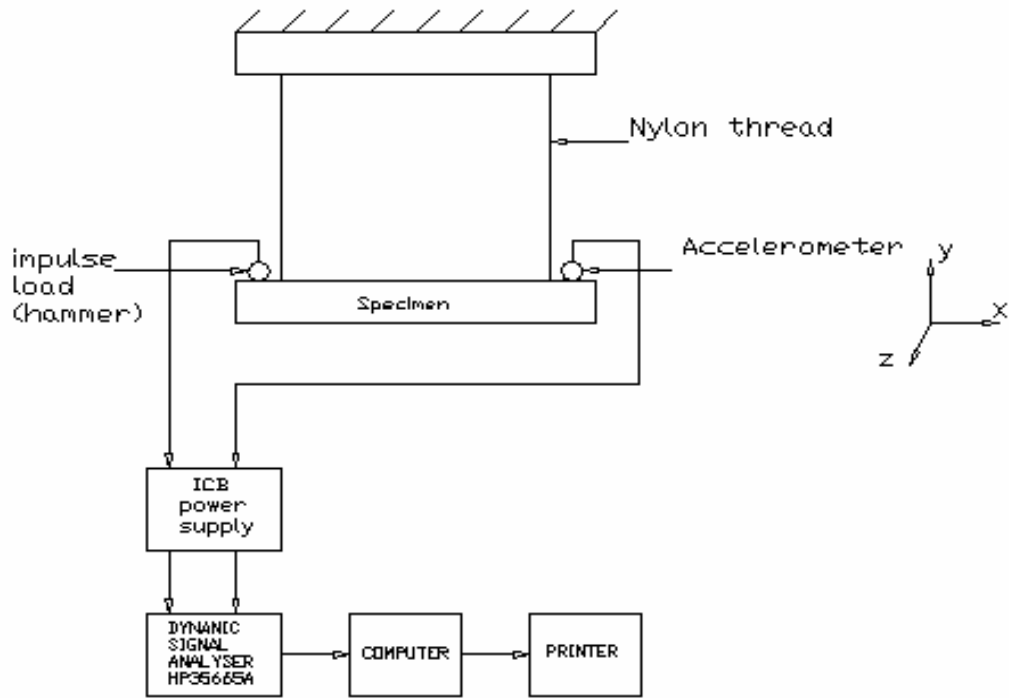


Figure 4.2 Schematic of the experimental setup (adapted from reference 19).

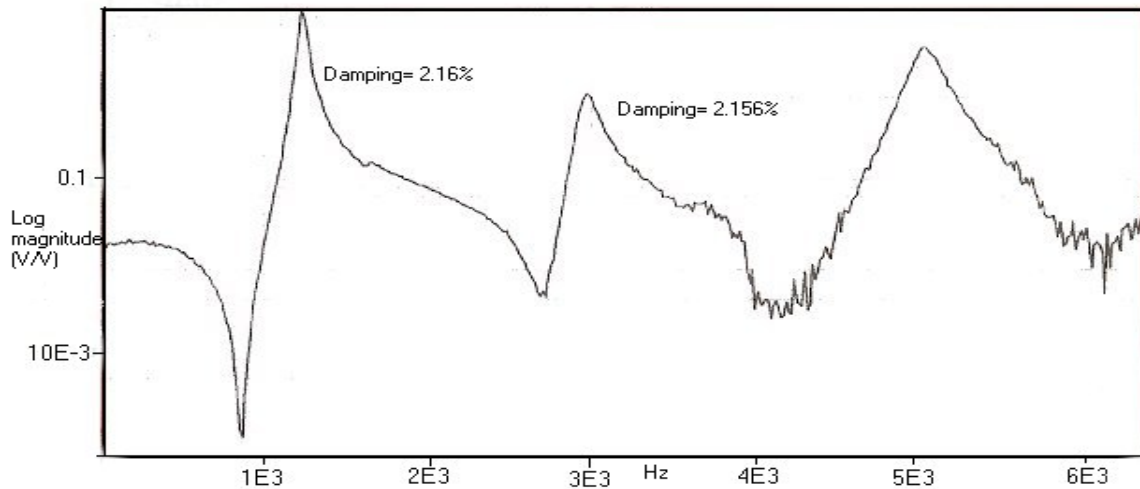


Figure 4.3 Typical frequency response function (adapted from reference 19).

For a beam of uniform cross section and uniformly distributed load with free-free boundary conditions, the natural frequency Φ_n is given:

$$\Phi_n = A \left(\frac{EI}{\mu L^4} \right)^{1/2} \text{ rad/sec} \quad (4.1)$$

where E = young's modulus
 I = moment of inertia,
 L = length of beam
 μ = mass per unit length of beam, and
 A = coefficient, 22.4 and 61.7, respectively for first and second modes

Once natural frequency is determined from the vibration test (modal analysis), Equation 4.1 may be employed in calculating Young's modulus, corresponding to the first/second mode.

4.4 Verification of Modal Analysis Test Methodology

A finite element (FE) model of the test beam 287 mm long was developed with 44 brick elements, employing PATRAN software. The beam was then analyzed by the ABAQUS program, Hibbet (Hibbet and Soreusch 1996), determining its eigen modes. The analysis required two material properties: Young's modulus and Poisson's ratio. The modulus input, 4400 MPa, was in fact the experimental modulus derived from the impulse frequency response test, with Poisson's ratio assumed to be 0.45. A comparison of natural frequencies from modal analysis with those from eigemode analysis reveals that the FE analysis satisfactorily predicts the first mode within 7% and 8% for control and precracked beams, respectively. There is hardly any agreement in the second mode frequency, due primarily to mesh sensitivity in the FE analysis. In view of the satisfactory agreement of the first mode frequency, it will be used in the modulus calculation.

4.5 Animation of Mode Shapes Employing ME'scopeVES

The experimental procedure and results were further authenticated by animating the measured deflection responses of the beam in slow motion, employing a ME'scope. Designed to observe and analyze vibration problems in structures and machines, it utilizes multichannel time or frequency domain data, acquired during the excitation of the beam. It displays operating deflection shapes and mode shapes at a moment in time or at a frequency, directly from the measured data. Though not included here for the sake of brevity, the observed mode shapes more or less agree with the theoretical predictions. In addition, the modal frequencies obtained from FRF plots are indeed verified with those indicated by deflection response of the beam.

4.6 Results and Discussion

Inducing different levels of precracking, three sets of beams (control and precracked) were tested. For discussion purposes, the ratio of loss in stiffness of the precracked beam to that of the control beam is referred to as damage. Accordingly, the three beams suffered damages of 9%, 12% and 18%. The trend lines in Figure 4.4 depict the (damage) recovery of the three beams. The first two beams, which received 9% and 12% damage by way of microcracks, recovered in 7 and 50 days, respectively. As expected, the more damage, the longer it took to recover. In contrast, the beam precracked to a higher damage level (18%) failed to recover even after two months. Note that this beam suffered some desiccation (1% weight loss) during the two-month period, though kept in a humidity room. It is unclear if the recovery process was hindered by the

marginal “cure.” Regardless, we assert that there exists a threshold level of damage, beyond which full recovery may be unattainable.

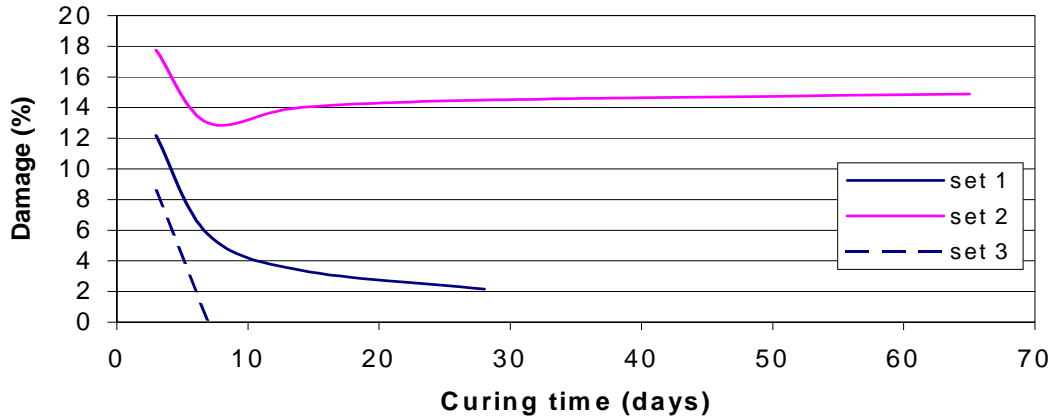


Figure 4.4 Healing in material with curing time. Damage is the ratio of loss in stiffness of precracked beam to the stiffness of control beam (adapted from reference 19).

The question now arises how the cracked beam with low modulus in the beginning caught up with its uncracked counterpart. As expected, the control beam had gained stiffness with time, but the cracked beam in a matter of days outpaced the control beam in attaining comparable stiffness. Cement hydration continuing for days and even months and resulting in the bonding of the aggregate matrix by calcium silicate hydrate (C-S-H) gel is the primary mechanism relating to long-term stiffness gain of cement treated soil. According to Jennings and Johnson (Jennings and Johnson 1986), the spherical cement particles (tricalcium silicate) are enveloped by hydration shells of C-S-H gel, whose thickness increases over time. The C-S-H gel formation is active in both uncracked and cracked materials, as is the calcium hydroxide crystal nucleation and growth in the continuum pore space. In precracked material, fresh calcium hydroxide also could permeate into existing microcracks, healing the cracks by bridging crack openings. It is this additional bonding that brought about the rejuvenation of the cracked beam, resulting in its stiffness attaining a level comparable to that of the control beam. In other words, both cracked and uncracked material benefited from continued gel formation and resulting cementing action. The precracked material, however, benefited more from nucleation of calcium hydroxide into crack openings.

4.7 Summary

Having observed that precracking the CTM had significantly improved its shrinkage cracking, it became important to ensure that the initial decline in stiffness modulus observed is temporary at best. Though field results revealed that the structural properties of the material were regained over time, a laboratory study under controlled conditions was undertaken looking into the recovery mechanism. Precracked and control beam specimens (287 mm long and 76 x 51 mm cross section) were subjected to modal analysis, extracting modal frequencies, and in turn, calculating Young’s modulus. Monitoring of beam stiffness clearly shows that precracked

material regained its stiffness with time, and length of recovery was governed by level of precracking or damage induced in the “young” material. Indications are that a threshold value of damage exists, beyond which full recovery may be unattainable. A plausible explanation for crack healing and/or recovery is offered by invoking the mechanism of nucleation of calcium hydroxide and C-S-H gel into the crack openings.

CHAPTER 5

SUMMARY AND CONCLUSIONS

Seeking materials and methods to alleviate shrinkage cracking in cement-treated soil, six test sections were constructed in August 2000. Extensive laboratory tests and field investigations were conducted during and after construction (for a period of 28 days) with the results reported in the first interim report dated April 21, 2001. After emplacement of 170 mm (6.75 in.) of hot mix asphalt (HMA) beginning September 21, 2000, the sections, still not opened to traffic, were monitored on November 14, 2001 (440 days). The third inspection and tests took place on June 16, 2003 (1034 days), which included deflection tests employing Falling Weight Deflectometer and a crack survey. The final field test program including FWD tests was conducted on December 1, 2004, and coring, DCP tests, and a crack survey were conducted on March 8, 2005 (1564 days). This final report not only presents the analysis results of the 1564-day tests, but also a comparative five-year performance of the two selected techniques (precut and precrack), two special additives-cement-fly ash and lime-GGBFS, and finally, the lime-fly ash mix, in mitigating shrinkage cracking and imparting long-term performance. Five and a half percent cement mix serves as a control for performance comparison.

5.1 Shrinkage Cracks

With a relatively thick HMA surface, the pavement remained crack-free once the experimental bases were overlaid on September 21, 2000. However, the 28-day crack results are convincing that the precracking technique is indeed effective in mitigating shrinkage cracks. For ready reference, the graph depicting the evolution of crack distress through the critical period of shrinkage and cracking of stabilized material is reproduced in Figure 5.1, which is adapted from reference 14. During the first 28 days, the cracks nearly reached a maximum in all of the sections, with the LFA section showing the least amount of crack (2.8%) and the precracked section a close second at 4.8%. As was shown, from a stiffness and strength point of view, LFA section performance is rated unsatisfactory, outweighing its best performance where shrinkage cracking is concerned. The precracked section exhibiting the least shrinkage crack potential is judged to be far superior to all other technique/stabilization additives. While reflective cracking could not be studied in this project for having placed a thick (222-mm [8.75-in.]) HMA layer, a recent study (Scullion, 2002) conducted at the Texas Transportation Institute is cited here to support the validity of precracking in mitigating reflective cracking. They concluded that the “microcracking or precracking proved quite effective at reducing reflective cracking,” which only complements the conclusions of the current study.

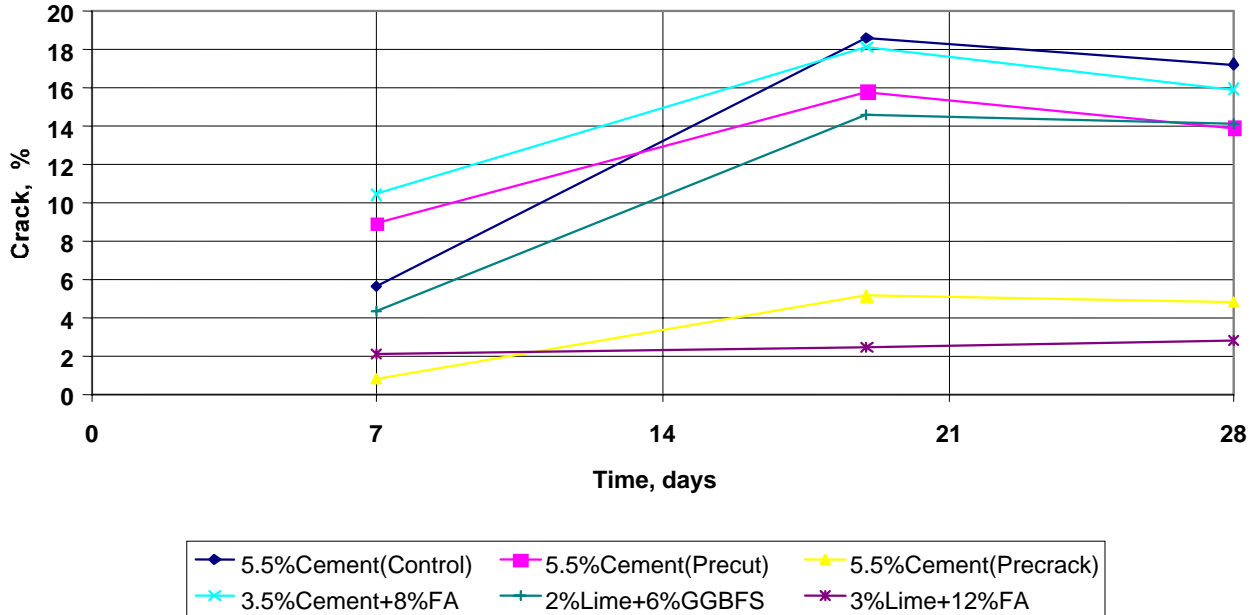


Figure 5.1 Evolution of crack density with time (adapted from reference 14)

5.2 Performance of Sections Based on Stiffness and Strength of Stabilized Soil

Stiffness of the pavement system governs the potential for deflection, and in turn, the overall performance of the system. Therefore, stiffness modulus of each stabilized layer (six test sections), is carefully compared to appraise the suitability of each of the six materials for short-term performance (shrinkage cracking) and long-term performance (deflection and consequent fatigue cracking). While evaluating a base material, a low initial stiffness is preferred in mitigating shrinkage cracking whereas it should attain a reasonably large stiffness 2000 – 2700 MPa (300 – 400 ksi) in the long run for structural performance. The stiffness results of six test sections are tabulated in Table 5.1. Table 5.1 rates the precracked section performing better than all of the other sections (both short-term cracking and long-term deflection performance), followed by precut and control sections. Since all of the three sections were treated with 5.5% cement admixture, and the fact the cost of microcracking is practically insignificant, precracking a “young” cement-treated base is by far an economical alternative for mitigating shrinkage cracks, and in turn, potential reflective cracking. From the stiffness point-of-view, however, all of the sections performed satisfactorily, except lime-fly ash section.

Table 5.1 Short-term and Long-Term Performance Compared and Rated

Section No.	28-day Modulus, MPa	440-day/1564-day Modulus, MPa	Short-term Cracking	Long-term Performance
1A, 3A	320	2710/3100	Good	Very good
1B, 3B	540	2240/3150	Good	Very good
2	410	2170/2820	Excellent	Very good
4	1530	1530/1500	Poor	Very good
5	2160	2160/2370	Poor	Very good
6	380	380/550	Very good	Poor

Strength of the stabilized material is important from the point of sustaining wheel loads, especially occasional overloads, without undergoing local deformation, manifested in the form of rutting and punching failure. With low strength throughout the five-year period, the LFA combination, based on the UCS test results in this program, is judged to be less suitable than all other five alternative treatments. Ultimate compressive strength of approximately 2070 kPa (300 psi) could be a target value for long-term performance.

The strength of the control cement mix (1730 kPa [250 psi] at 1564 days), with practically no gain from 1034 to 1564 days (1670 kPa [240 psi] to 1730 kPa [250 psi]) raises some concern as to its suitability for long-term performance. Put differently, the CTM of the 7-day design strength of 2070 kPa (300 psi) performed marginally at best. Though CFA and LGBFS materials fulfilled the strength requirements, the additional cost of incorporating a secondary additive and potential mixing nonuniformity outweigh the benefits, if any, in comparison to a single additive, such as cement. Inferred from this discussion is that a low-strength cement mixture with certain field modification such as precracking or precutting could serve well to produce a satisfactory stabilized base. The added cost combined with the logistics of precutting, however, would make this option a less desirable alternative. By the process of elimination, therefore, the precracking technique emerges as the economically feasible and effective technique to alleviate shrinkage cracking, and, in turn, reflective cracking.

5.3 Overall Conclusions

Investigations during construction and evaluation tests thereafter for a period of five years reveal that large variation in compaction and moisture is real, attributable to inherent difficulties of in-place mixing and compacting. Owing partly to inadequate mixing, field-mixed material strength on average was 50% lower than that of the laboratory-mixed material. Mix nonuniformity was pronounced when two additives were employed, for example, a cement and fly ash combination. It was discovered while coring that the lower reach of the stabilized section was deficient in stabilizer chemical, which only caused partial disintegration of core samples. The low modulus of CFA over the five-year period (except the 28-day value), and the slightly larger FWD deflection are cited here in support of this premise. The strength gain over the monitoring period of all of the sections was satisfactory, with the exception of the cement control section, whose 1564-day UCS turned out to be 1730 kPa (250 psi), falling short of the design strength, 2070 kPa (300 psi).

An overall comparison of the performance of all of the sections based on shrinkage cracking (referred to as short-term performance), and stiffness and strength (signifying long-term performance) is presented in Table 5.1. Judging short-term performance in terms of 28-day cracks, sections 2 and 6 have outshined the other four sections. Indeed, sections 1, 3, 4 and 5 suffered excessive shrinkage. The long-term performance of the LFA section is suspect, as evidenced by its relatively large deflection, due in part to the LFA base not attaining the expected strength/stiffness. Though the shrinkage cracking of the CFA section was excessive, and the FWD deflection of the section slightly larger than that of the control section, its structural performance so far is on target. Mixing problems in incorporating two admixtures and the attendant weakness of the base layer could have been the primary reasons for the enhanced deflection. This mixing problem existed in the lime-GGBFS mixture as well; nonetheless, its adverse effect on strength and stiffness seems to be minimal. The use of these two mixtures – CFA and lime-GGBFS – is deferred until the shrinkage cracking problem is addressed adequately.

The three remaining admixtures/treatments include the low-strength cement-treated material (5.5% cement admixture), an identical CTM receiving precutting during construction, and again the same cement admixture subjected to precracking 24 hours after completion of construction. The 5.5% cement mixture, designated the control mix, not only suffered excessive shrinkage cracking (17.2%) but also its long-term strength gain fell short of expectations. The precut cement mixture, though structurally sound with adequate long-term strength, underwent shrinkage cracking of 13.9%, which is considered excessive. From the point of view of overall performance, precracked material indeed excelled over all of the other treatments/admixtures.

5.4 Recommendations

The results of the study show that the stabilized base layers perform satisfactorily if the overlying HMA is sufficiently thick (more than 152 mm [6 in.]). If the HMA layer is 102 mm (4 in.) or less, early shrinkage cracking becomes an issue and should be addressed. Toward this end, early strength (7-day strength) should be limited to 2070 kPa (300 psi) in conjunction with some form of conditioning implemented in the constructed layer. Of the two conditioning techniques experimented with in this study, precracking the stabilized cement layer was highly successful and therefore recommended for implementation. Tentative specifications for constructing precracked CTM layers have been developed by the Texas Transportation Institute, which may be referred to for guidance (Scullion, Sebesta, Harris and Syed 2000). The performance of the other section with precut was not entirely satisfactory. Considering the complexity of implementing this procedure, precutting the freshly laid cement layer cannot be recommended at this time.

Cement-fly ash not only failed to show improvements in shrinkage cracks, but gain in bending strength as judged by elastic modulus suffered as well, due in part to nonuniform mixing of additives. This combination of two admixtures, therefore, cannot be recommended. The shrinkage cracking performance of the lime-GGBFS combination was less than satisfactory; however, the structural performance of the mix was deemed above average. Its use, therefore, could be promoted should the design warrant a thick HMA layer. As precracking this material is likely to alleviate shrinkage cracking problems, a recommendation would be to conduct a study incorporating this feature in lime-GGBFS material with its adoption conditional upon the success of the project. Very effective in mitigating shrinkage cracks and also being able to preserve long-

term strength and stiffness, the precracked CTM (7-day strength - 2070 kPa [300 psi]) emerges as a clear choice for pavement applications.

ACKNOWLEDGEMENTS

The research reported in this paper (PCA R&D Serial No. 2581) was conducted by Hiteck Engineering Consultants with the sponsorship of the Portland Cement Association (PCA Project Index No. 00-02). The contents of this report reflect the views of the author, who is responsible for the facts and accuracy of the data presented. The contents do not necessarily reflect the views of the Portland Cement Association.

During the period of this study, the State Research Engineer was Joy Portera followed by Randy Battey. Bill Barstis and M. Howard of MDOT helped to organize the field work. Field data collection was under the direction of Johnny Hart. Special thanks to Jackie Harris, the project engineer, and Danny Walker, the Assistant District Engineer. The support of Portland Cement Association and that of Holman, Inc., (Tim Cost) is acknowledged here.

Several graduate students were involved in the project data collection, including A.M. Rahim, Upendra Joshi, and Biplab Bhattacharya. Sherra Jones ably typed all of the reports.

REFERENCES

George, K.P., *Final Report on the Study of Criteria for Strength and Shrinkage Control of Cement-Treated Bases*, University of Mississippi, University, Mississippi, USA, May 1968.

Bofinger, H.E.; Hassan, H.O., and Williams, R.I.T., *The Shrinkage of Fine-Grained Soil-Cement, TRRL Supplementary Report 398*, Transport and Road Research Laboratory, Crawthorne, England, 1978.

Scullion, T.; Sebesta, S.; Harris, J.P., and Syed, I., *A Balanced Approach to Selecting the Optimal Cement Content for Soil-Cement Bases*, Report 404611-1, Texas Transportation Institute, College Station, Texas, USA, 2000.

Reflective Cracking in Cement Stabilized Pavements, IS537, Portland Cement Association, Skokie, Illinois, USA, 2003.

Colombier, G. and Marchand, J.P., "Precracking of Pavement Underlays Incorporating Hydraulic Binders," *Proceedings of the 3rd International RILEM Conference on Reflective Cracking in Pavements*, The Netherlands, E & FN Spon., 1996.

Shahid, M.A. and Thom, N.H., "Performance of Cement Bound Bases with Controlled Cracking," *Proceedings of the 3rd International RILEM Conference on Reflective Cracking in Pavements*, The Netherlands, E & FN Spon., 1996.

Lefort, M., "Technique for Limiting Consequences of Shrinkage in Hydraulic-Binder Treated Bases" *Proceedings of the 3rd International RILEM Conference on Reflective Cracking in Pavements*, The Netherlands, E & FN Spon., 1996.

Yamanouchi, T., and Ihido, M., "Laboratory In-Situ Experiments on the Problem of Immediate Opening of Soil-Cement Base to General Traffic," *Proceedings of the 4th Australia-New Zealand Conference*, 1982.

Teng, T.C., and Fulton, J.P., "Field Evaluation Program of Cement-Treated Bases," *Transportation Research Record*, 501, Washington, D.C., USA, 1974, pages 14 to 27

Litzka, J., and Haslehner, W., "Cold In-Place Recycling on Low-Volume Roads in Austria" *Proceedings, 6th International Conference on Low Volume Roads*, Minneapolis, Minnesota, USA, June 1995.

Brandl, H., "Mixed in Place Stabilization of Pavement Structures with Cement and Additives," *Proceedings of the XIIth European Conference on Soil Mechanics and Geotechnical Engineering*, Rotterdam, Netherlands, 1999.

Scullion, T. and Saaverketo, T., "Precracking of Soil-Cement Bases to Reduce Reflection Cracking," *Transportation Research Record* 1787, Washington, D.C., USA, 2002.

Sebesta, S., Use of Microcracking to Reduce Shrinkage Cracking in Cement-Treated Bases, *Presented at the 84th Annual Meeting, Transportation Research Board*, Washington, D.C., USA, 2005.

George, K.P., *Soil Stabilization Field Trial (Interim Report I)*, Department of Civil Engineering, The University of Mississippi, University, Mississippi, USA, April 2001.

George, K.P., *Soil Stabilization Field Trial (Interim Report II)*, Department of Civil Engineering, The University of Mississippi, University, Mississippi, USA, February 2002.

George, K.P., *Soil Stabilization Field Trial (Interim Report III)*, Department of Civil Engineering, The University of Mississippi, University, Mississippi, USA, November 2003.

Lukanen, E.O.; Stubstad, R., and Briggs, R., *Temperature Predictions and Adjustment Factors for Asphalt Pavement*, Report No. FHWA-RD-98-085, Braun Intertec Corporation, Minneapolis, Minnesota, USA, June 2000.

Barstis, B.F., *Long-Term Effect of Lime-Fly Ash Treated Soils*, FHWA/MS-DOT-RD-03-147 Mississippi Department of Transportation, Jackson, Mississippi, USA, December 2003, page 333.

George, K.P.; Brajacharya, M., and Gaddam, M., "Precracking Mitigates Shrinkage Cracking in Cement-Treated Material," *Proceedings of the Damage and Fracture Mechanics Conference*, 2002, WIT, Southampton, U.K., 2002.

Hibbet, K., and Soreusch, Inc., "Getting started with ABAQUS/STANDARD," version 5.5, 1996.

Jennings, H.M., and Johnson, S.K., "Simulation of Microstructure Development During the Hydration of Cement Compound" *American Ceramic Society*, 69, 1986, pages 790 to 795.

McElvancy, J., and Djatinka, IR.B., "Strength Evaluation of Lime-stabilized Pavement Foundation Using the Dynamic Cone Penetrometer," *Journal of Australian Road Research Board*, Vol. 21, No. 1, March 1991.

Jianzhou, C.; Mustaque, H., and LaTorella, T.M., "Use of Falling Weight Deflectometer and Dynamic Cone Penetrometer in Pavement Evaluation," *Transportation Research Record 1655*, National Research Council, Washington, D.C., USA, 1999.

APPENDIX A

PROCEDURE FOR BACKCALCULATING LAYER MODULI EMPLOYING ELMOD

A step-by-step procedure adopted for backcalculating layer moduli from deflection bowls which seemingly resulted in unrealistic moduli:

- Step 1. Accessing ELMOD program click on STRUCTURE menu.
- Step 2. Input in the appropriate boxes layer thicknesses and E_3/E_4 ratio (E_3/E_4 ratio is preferred over E_2/E_3). No need to enter seed moduli.
- Step 3. Click OK and access MODULI menu.
- Step 4. Select DEFLECTION BASIN FIT; fix E_4 by checking the box; enter the tolerance RMS value in the box labeled STOP WHEN RMS <...., and click on CALCULATE.
- Step 5. Evaluate the reasonableness of the output moduli, assessing how they fit chronologically with previous stiffness values and also spatially within a uniform section.
- Step 6. If the resulting moduli do not fit the desired trend, change the E_3/E_4 ratio and rerun the program until the analysis results in “reasonable” values.

APPENDIX B

In order to apply temperature correction to moduli value, a two-step procedure needs to be followed:

1. Predict the temperature at the mid-depth from surface temperature time of test and average air temperature (°C) the day before testing. BELLS3 method (17), developed in connection with LTPP testing is employed for this purpose. The following equation is solved to obtain pavement temperature at mid-depth:

$$T_d = 0.95 + 0.892 * IR + \{\log(d) - 1.25\} \{-0.448 * IR + 0.621 * (1\text{-day}) + 1.83 * \sin(hr_{18} - 15.5)\} + 0.042 * IR * \sin(hr_{18} - 13.5) \dots \dots \dots B-1$$

where:

- T_d = Pavement temperature at depth d, °C
- IR = Infrared surface temperature, °C
- Log = Base 10 logarithm
- d = Depth at which mat temperature is to be predicted, mm
- 1-day = Average air temperature (°C) the day before testing
- sin = sine function on an 18-hr clock system, with 2π radians equal to one 18-hr cycle
- hr_{18} = Time of day on a 24-hr clock system, but calculated using an 18-hr AC temperature rise- and-fall time cycle

2. For temperature adjustment of backcalculated asphalt moduli, the following equation is employed:

where: $ATAF = 10^{(\text{slope} * (T_r - T_d))} \dots \dots \dots B-2$

- ATAF = Asphalt temperature adjustment factor
- slope = Slope of the log modulus versus temperature equation
(-0.0195 for the wheelpath and -0.021 for mid-lane are recommended)
- T_r = Reference mid-depth hot-mix asphalt (HMA) temperature, °C
- T_d = Mid-depth HMA temperature at time of measurement, °C

Note: Most of the slopes range between -0.010 and -0.027 (a reasonably broad range). The most common occurring slopes are -0.0195 for tests taken in the wheelpaths and -0.021 for tests taken mid-lane.